REPORT DOCUMENTATION PAGE

Form Approved OMB No. 0704-0188

1. AGENCY USE ONLY (Leave blank)	2. REPORT DATE	3. REPORT TYPE AND DATES COVERED
	1998	Final Report

4. TITLE AND SUBTITLE

Spontaneous Ignition of Hydrocarbon Fuels at Temperatures in the Range 750-1500K

5. FUNDING NUMBERS

F61775-98-WE103

6. AUTHOR(S)

Prof. John Frederick Griffiths

7. PERFORMING ORGANIZATION NAME(S) AND ADDRESS(ES)

The University of Leeds
School of Chemistry
Leeds LS2 9JT
United Kingdom

8. PERFORMING ORGANIZATION REPORT NUMBER

N/A

9. SPONSORING/MONITORING AGENCY NAME(S) AND ADDRESS(ES)

EOARD
PSC 802 BOX 14
FPO 09499-0200

10. SPONSORING/MONITORING AGENCY REPORT NUMBER

SPC 98-4072

11. SUPPLEMENTARY NOTES

12a. DISTRIBUTION/AVAILABILITY STATEMENT

Approved for public release; distribution is unlimited.

12b. DISTRIBUTION CODE

A

13. ABSTRACT (Maximum 200 words)

This report results from a contract tasking The University of Leeds as follows: The contractor will investigate methods for enhancing the initiation of combustion in hydrocarbon fuels as outlined in his proposal submitted in April 1998.

14. SUBJECT TERMS

EOARD, Fuels, Kinetic Theory, Combustion

15. NUMBER OF PAGES

59

16. PRICE CODE

N/A

17. SECURITY CLASSIFICATION OF REPORT	18. SECURITY CLASSIFICATION OF THIS PAGE	19. SECURITY CLASSIFICATION OF ABSTRACT	20. LIMITATION OF ABSTRACT
UNCLASSIFIED	UNCLASSIFIED	UNCLASSIFIED	UL

SPONTANEOUS IGNITION OF HYDROCARBON FUELS AT TEMPERATURES IN THE RANGE 750 - 1500 K

J.F. Griffiths
School of Chemistry
University of Leeds
Leeds LS2 9JT, UK

Contract No. F61775-98-WE103

CONTENTS

ABSTRACT

There is a need to develop methods for the initiation of combustion in scramjets which are reliable, flexible in operation over wide ranges of conditions and which do not require excessive ancillary equipment on board the device. The optimum method would be to utilise spontaneous ignition of the fuel at the launching conditions, if necessary with some enhancement of reactivity. In order to achieve this goal it is first essential to understand the combustion chemistry of typical fuel components which bring about spontaneous ignition, in order to establish what may or may not be possible.

The purpose of this review is to establish the chemical principles and detailed kinetics which underlie the spontaneous ignition of hydrocarbons and determine the ignition delay, to assess sources of information and experimental methods involved, and to explore the scope for the initiation enhancement within appropriate ranges of conditions.

1. AUTOIGNITION TEMPERATURES AND IGNITION DELAY TIMES

In order to discuss ways in which the spontaneous ignition of scramjet fuels may be enhanced it is important to be able to understand and interpret the reactivity of different classes of hydrocarbons. One measure of reactivity is the minimum temperature at which a fuel vapour + air mixture is able to undergo spontaneous ignition in a closed vessel, the autoignition temperature (AIT). The duration of the ignition delay of one fuel relative to that of another in identical circumstances is also a measure of the reactivity of the fuel, and it is the property of most direct relevance to initiation of ignition in scramjets.

1a Autoignition temperatures

The minimum autoignition temperatures (the AIT) of flammable vapours are determined in a prescribed way by internationally established test procedures (ASTM-E 659-78, BS 4056, EC - L 251/84). The pre-requisite is a fixed volume vessel which is uniformly heated in an oven (200 cm^3, conical flask in the BS and EC test). The flask is open to the atmosphere so that constant (atmospheric) conditions are maintained. It is purged with air prior to each experiment. The vessel is controlled at a preset temperature and liquid fuel is injected into the flask. Whether or not ignition occurs is determined by visual observation. The vessel temperature is then varied and the experiment is repeated until the minimum temperature at which spontaneous ignition is possible is established. The test does not specify a particular composition of the fuel vapour + air mixture. Ignition will occur in the most reactive mixture as an automatic response as the injected liquid vaporises and mixes with the air.

This test procedure establishes the relative reactivities of different compounds and their isomeric structures. Whilst the AIT for different fuel components also gives a useful indication of the temperature at which exothermic oxidation becomes significant, a limitation of the information is that there is no indication of how the autoignition temperature may vary in different sizes and shapes of reactor or when the pressure is changed. The measured AITs of a range of compounds from different classes of hydrocarbons are given in an Appendix.

1b Ignition delay

The ignition delay (τ) is defined as the time interval from the start of events, such as the introduction of a fuel or fuel + oxidant mixture to the system to the occurrence of flame or some other manifestation of ignition. Suitable quantitative monitors of the ignition event could be the maximum in light output, or other spectroscopic data, or the maximum rate of temperature or pressure change in a closed system. Ignition delays may be measured in closed vessels, shock tubes or rapid compression machines. These experimental techniques are discussed in Section 2.

Provided that premixed gaseous fuels are used, the ignition delay arises solely from the development of the heat release rate in the chemical process in competition with the heat loss rate from the system. Although these also influence the ignition delay during droplet combustion, they are not the only factors [Goodger

and Eissa (1987)]. Liquid evaporation and mixing may contribute to the overall elapsed time before ignition occurs when droplets are injected into heated gases, and they may even be the most important factors if the chemical timescale is short compared with the "physical" timescale. If kinetic interpretations are being sought, it is important to limit the analysis to a range of conditions in which the reaction is under kinetic control.

At initial temperatures above about 850 K, ignition of all hydrocarbons develops in a single stage (Fig. 1). At lower initial reactant temperatures a two-stage ignition can be discerned from the pressure record during alkane ignition, and that of other organic compounds in closed systems (Fig. 2). These examples were obtained from studies in a rapid compression machine. Exceptionally, methane, ethane, ethene, and the simple aromatic fuels do not show the two-stage reaction and they do not readily undergo spontaneous ignition at temperatures below about 750 K.

The first stage of a two-stage ignition involves the development of a "cool flame". This gives a modest pressure increase in a closed vessel, which signifies that some heat release has occurred and the reactant temperature has increased because of it, typically to 800 - 850 K. The rate of pressure change is deceleratory, such that a temporary "plateau" is often observed in the pressure record (Fig. 2). The time from initiation of reaction (marked as the end of compression in Fig. 2) to the maximum rate of pressure rise in the first stage, which corresponds to the maximum in an accompanying light output, is defined as τ_1. The interval from this point to the maximum rate of pressure rise in the second stage is defined as τ_2. When the variation of these parameters is plotted as a function of the isentropically compressed core gas temperature (see Section 2) it is found that τ_1 decreases monotonically with increasing temperature, whereas τ_2 increases at first, before decreasing (Fig. 3). The overall consequence is that the ignition delay τ ($= \tau_1 + \tau_2$) decreases at both low and high compressed gas temperatures, but exhibits an intermediate temperature range within which τ increases. The origin of this complex dependence of τ on the control temperature (the initial, or compressed gas temperature in this case), can be traced back to the kinetic mechanisms involved and how they are affected by temperature (Section 3).

It is possible for the ignition delay at a given reactant density and control temperature to be reproduced quantitatively in different systems, but only under adiabatic conditions. When heat losses occur, the measured ignition delay at given conditions is a characteristic of the experimental system. For a particular reactant composition and density, even the range of control temperatures in which a negative temperature dependence of ignition delay is measured varies from system to system.

The magnitudes of ignition delays for various fuels under a range of conditions in are shown in Figs 4 - 6. These examples are confined to conditions which may be close to adiabatic. The results for n-heptane (Fig. 4 and 5) originate from ignition behind an incident shock [Ciezki and Adomeit (1993)]. Although it is not a point of relevance in the present Section, the solid lines through the experimental data points in Fig. 4 relate to the application of an abbreviated kinetic model for the simulation of the ignition delay [Poppe *et al* (1994)]. The experimental results obtained by Ciezki and Adomeit [1993] have been used by a considerable number of workers to validate

the predictions of numerical models to simulate n-heptane combustion. The comparison made in Fig. 4 appears to be the only one in which the extent of the scatter on the experimental results is fully exposed.

Higher hydrocarbons are studied invariably by injection of fuel droplets into a system. Thus evaporation may contribute to the elapsed time to ignition. This may be contributory to the ignition delay of n-tetradecane measured by Cavaliere *et al* [1993] by the "diesel injection" of a droplet spray into hot, flowing air (Fig. 5). The results displayed by the authors [Cavaliere *et al* (1993)] as a wholly irrational log t versus 1/T graph have also been re-interpreted in Fig. 5 in terms of "real money". The ignition delays obtained by Goodger and Eissa [1987] were measured from the injection of a single falling drop into a heated enclosure (Fig. 6). Almost certainly these measured times are dominated by droplet heating and evaporation since the ignition delays for n-heptane are about two orders of magnitude longer than those of Ciezki and Adomeit [1993] for pre-mixed fuel + air at comparable pressures (Fig. 4). Even the ignition delays for n-tetradecane, obtained by Cavaliere *et al* [1993], are an order of magnitude shorter than those for n-heptane measured for a single, large drop (cf Figs. 5 and 6). Whilst droplet injection was necessary for the study of toluene ignition behind a reflected shock (Fig. 7), it is probable that evaporation had occurred following passage of the incident shock [Cadman (1993)]. Measurements from extensive studies of ignition delays in the former Soviet Union are reported by Sokolik [1963].

2. EXPERIMENTAL METHODS

2a Closed, constant volume reaction vessels

Experiments in closed, constant volume vessels involve admission of reactants to an evacuated vessel. The vessel is maintained at constant temperature in an oven so that an experiment is performed at a given initial reactant pressure (p) and vessel temperature (T_a). Glass systems can be used at pressures below one atmosphere. Pyrex glass is satisfactory if the control temperature is not taken above 750 K, otherwise Silica is required. Optical access within the visible transmission range also presents no problem with glass vessels. Metal vessels (normally stainless steel) are required for experiments at atmospheric or higher pressure. There may be difficulties with surface activity in such cases, although glass vessels are not entirely free of such problems.

Many of the studies of hydrocarbon ignition that were made in the 1930s were performed in steel vessels at high pressures, mainly because the combustion in air was studied [Lewis and von Elbe (1978)]. The ($p - T_a$) ignition diagrams for many different fuels, which delineate the conditions at which spontaneous ignition and cool flames of the fuel vapour + air occur, were established at this period. Later (1950 - 1970) it became more fashionable to work with fuel + oxygen mixtures at sub-atmospheric pressures in closed vessels. Whilst fundamentally important to the understanding and interpretation of hydrocarbon oxidation, these studies are of a less direct relevance to practical applications where combustion takes place in air [Griffiths and Scott (1987)].

Pressure and temperature changes are normally measured by transducer and by thermocouples respectively, and the global light output may be detected by a photomultiplier. The moment of ignition is easily identified by any of these methods, and the ignition delay, from the gas entry time, is accurately measured.

2b Flow systems

Flow systems may be classified as heated laminar tubes, or plug flow tube reactors, (PFTR) and burners, or heated turbulent flow reactors and well-stirred, or continuous stirred-tank reactors (CSTR).

Laminar flow tubes

Heated laminar flow tubes operated at atmospheric pressure, were used in some of the earliest chemical studies of hydrocarbon oxidation [e.g. Pease (1929), Beatty and Edgar (1934)]. Premixed gaseous fuel and air are flowed through a heated tube. The system lends itself particularly well to continuous gas sampling and chemical analysis. Ignition delays may be inferred through the flow rate and the appearance of ignition, if a flame can be stabilised, but the effect of temperature change on the flow rate must be taken into account.

Vertical, upward flow, laminar flow reactors which have been used to study stabilised cool flames and two-stage ignitions were pioneered at the Naval Research Laboratories in Washington [Williams *et al* (1959)]. The stabilisation of a cool flame and two-stage ignitions in tubes were reported in earlier work also, but usually with a horizontal orientation, which gave rise to considerable distortion of the combustion fronts, as a result of buoyancy effects which disturbed the horizontal, laminar flow [Spence and Townend (1949)].

Leeds laminar flow system

A flow rig is in use at Leeds University which was designed specifically to characterise the reactivity of diesel fuels at atmospheric pressure and to measure the performance of ignition enhancers [Rocha (1996)]. It is shown schematically in Figure 8 and described in some detail below, because this gives some background on how enhancement of ignition may be assessed.

The continuous flow rig consists of a quartz tube with an internal diameter of 18 mm and total length of 1020 mm through which is passed a pre-heated carrier gas and where fuel and atomisation air (or nitrogen) are then injected into the carrier gas. The tube is surrounded along its length by four heating jackets namely pre-heater, zone I heater, zone II heater and zone III heater. The tube is not heated in the fuel injection section, but it is enclosed by a thermal insulation with fibreglass to minimise the heat loss. The heating jackets combined with the thermal insulation permit the stabilisation of a reasonably uniform temperature throughout the flow rig under test conditions.

The air (or nitrogen) flow is divided into primary flow for atomisation and secondary flow, namely pre-heater feed. Both the primary and secondary air (or nitrogen) flows are controlled by means of a solenoid controlled flow valves. Total

flow rates of up to 200 $cm^3 s^{-1}$ correspond to residence times of about 5 ms cm^{-1}. The liquid fuel injection is controlled by means of a continuous infusion syringe pump to keep a constant volumetric flow into the rig through a fuel injector nozzle. The infusion syringe has a data interface which is controlled by an external computer.

The control of the temperature is obtained by four thermoelectric sensors fitted to the heaters which allows independent control of each furnace zone. Additional thermocouples are also fitted at the position of the inlet air (or nitrogen) to preheat feed and at the probe tip. Each thermocouple is connected to a communicating controller. The sensors have an analogue output. The data processing is accomplished with an on-line computer.

An automatically controlled, gas sampling probe is also fitted with a thermocouple at its tip. The probe movement and position is controlled by means of an automatic carrier with integral ball screw driven by a small electric motor fitted at the end of the probe rod. Gas sampling is undertaken at reduced pressure. Carbon monoxide and carbon dioxide are measured by means of infrared absorption devices connected to vacuum pumps. The sampled gases are first passed through a cooling chamber to condense and separate any unreacted fuel and condensable products. Oxygen is measured by means of a paramagnetic analyser also connected to a vacuum pump.

The temperature controllers, the air (or nitrogen) flows, the syringe pump flow, the probe carrier and the gas analysers are connected to a microprocessor-based automated data acquisition system which includes the data logger and the pc-based data acquisition system (Fig. 9). The data-logger is a microprocessor-based device to collect and store signal received by transducers (e.g. thermocouples) which convert the physical variables of interest into electric signals. There is also an analogue display of the operating mode and conditions of the system. A typical example of the automated data acquisition print-out is shown in Figure 10. The furnace zones were set so that as near a constant temperature as possible was achieved along the length of the tube under non-reactive flow conditions, the "baseline" temperature. This varied about the mean by +/- 10 K at different points along the tube. The gas analysers were not being operated in the example shown in Fig. 10.

In operation, the system automatically performs an initial cycle without any fuel flow, to establish a baseline temperature profile with the set air or nitrogen flows. The fuel is then switched on and the same cycle is traversed. This includes the probe being held for a prescribed interval (the "dwell time") at each of the designated sampling positions. The output indicated as "temperature difference" represents the difference between the temperatures measured at each point in a reactive and non-reactive experiment. The shape of the ΔT - position profile is fundamentally important, but a useful initial screening arises from the residence time at which $\Delta T = 0$ (Fig. 11). This is represented in Fig 10 as the "ignition delay time", and marked as "point A" on Fig. 11, although ignition has not actually occurred. In fact, a more appropriate monitor of the reactivity of a given mixture emerges from a comparison between the reactive temperature profile, and a profile determined with the fuel being atomised into a nitrogen flow equivalent to that of air under reactive conditions. This takes full account of the enthalpy requirement for vaporisation of the fuel. The

representative results, showing the enhancement of the combustion of 1-octene by small proportions of di-t-butyl peroxide (Fig. 12) and by isopropyl nitrate (Fig. 13), were obtained in this way. A comparison with n-heptane is also included. These results are plotted in terms of the reactant temperature difference as a function of position relative to the temperature in a non-reactive flow. The baseline temperature (i.e, without fuel injection but with inert gases at the same total flow rate) was in the range 675 - 695 K throughout the length of the tube.

Well-stirred flow reactors

CSTRs and turbulent flow reactors have been operated mainly at pressures from 1 - 10 bar, with residence times varying from many seconds to less than 100 ms at the highest operating pressures. In most cases the reactants are mixed after metering and pre-heating, and then flow through the reactor at constant pressure and flow rate. The reactor temperature may be held constant, or it may be varied continuously or in a stepped manner, in order to probe the modes of behaviour for a given fuel + oxidant composition over the temperature range.

A well-mixed condition can be established in the CSTR by either a mechanical stirrer [Caprio *et al* (1981), Gray *et al* (1984)] or jet mixing of the gases [Lignola *et al* (1983), Dagaut *et al* (1994)]. The former is required when mean residence times in the reactor exceed a few seconds, since jet velocities are then too low to sustain reasonable spatial uniformity. Surface effects have been minimised by Dagaut *et al* [1994], in their high pressure kinetic studies in a jet-stirred flow system, by surrounding a silica vessel with a stainless steel pressure chamber. Different modes of operation of CSTRs are reported. The studies by Dagaut *et al* [1994] in a 35 cm^3 CSTR were designed for isothermal chemical measurements at high pressures. Very high dilutions with N_2 were employed so that temperature changes within the reactants during exothermic reaction were minimised. The investigations of non-isothermal phenomena at high pressures, by Lignola *et al* [1988], were performed in stoichiometric mixtures of fuels in air in a larger CSTR (100 cm^3). Kinetic studies in a well-stirred flow reactor by Malte and co-workers at the University of Washington [Thornton *et al* (1986), Westbrook *et al* (1988)] apply to temperatures in excess of 1000 K.

Turbulent flow reactors

A turbulent flow reactor, at Princeton University, has been operated at atmospheric pressure over many years to give information on the detailed chemistry of hydrocarbon oxidation in the temperature range 1000-1200K. Aromatic compounds as well as alkanes and alkenes have been investigated [Dryer and Glassman (1973), Venkat *et al* (1982), Brezinsky *et al* (1984, 1986), Brezinsky (1986), Dryer and Brezinsky (1986a, 1986b), Emdee *et al* (1990), Shaddix *et al* (1992)]. Constant molar proportions, $RH:O_2:N_2$, are established at the inlet, usually with a fuel:oxygen ratio close to $\Phi = 1.0$ but with a high dilution by nitrogen. Very high gas flows are maintained so that radial gradients are eliminated by turbulence, leading also to short contact times ($t < 200$ ms). Operation of the tube is regarded to be virtually adiabatic and axial temperature increases of up to 200 K occur as the reactants progress along the tube. A turbulent, high pressure, flow reactor has been

developed by Koert *et al* [1994] for studies of propane combustion throughout the temperature range from 600 to 1000K and at pressures up to 1.5 MPa.

Heated, flat flame burners also have been used for the stabilisation of cool flame and two-stage ignitions. These systems were pioneered by Agnew *et al* [1957], and a definitive study of the spatially resolved chemistry of diethyl ether combustion has been reported [1965]. Ballinger and Ryason [1971] have described this type of burner in detail and have reported the relative behaviour of some n-alkanes, primary reference fuel mixtures, and the effect of anti-knock additives. Whether or not such a system could be used to investigate the performance of ignition promoters has not yet been explored.

An important application of the heated, flat flame burner is the photolytic perturbation of the post cool flame gases downstream from the stabilised cool flame of n-heptane [Morley (1988)]. The chemical perturbation was initiated by an incident laser beam which dissociated H_2O_2 to OH radicals. The relaxation of the excess OH, measured by laser induced fluorescence, was shown to be tied to the principal reaction modes in alkane oxidation, namely propagation, termination and net branching. Global rate parameters were quantified from the decay curves.

Carlier *et al* [1990] stabilised the two-stage spontaneous ignition of n-butane on a heated flat flame burner at a pressure of 0.18 MPa. The temperature profile was measured by a chromel-alumel coated thermocouple and samples at different points along the axis of the reactor were removed for analysis by gas chromatography, polarography or electron spin resonance (esr) spectroscopy. The esr signals gave information about the spatial variation of HO_2 and RO_2 radical concentrations.

2c Shock tubes

Ignition delays over very wide ranges of temperature and pressure can be measured from the study of combustion behind a shock wave under controlled experimental conditions in a shock tube. If the response under virtually adiabatic conditions is required then a practical, minimum, shock temperature is about 1000 K, for which ignition delays are unlikely to exceed a few milliseconds at the shocked gas pressure. Heat loss is possible if the ignition delay is longer than this, which is likely to be the case at lower temperatures. The near discontinuity in temperature that is achieved when the shock passes through the reactants gives a very well defined start to the reaction, from which an ignition delay can be well-characterised. There can be complications in other types of closed, experimental systems because gas admission or heating rates can occur on a timescale that is comparable with the chemical timescale.

Typically the shocked gas temperatures for ignition delay measurements fall in the range 1500 - 2500 K [Burcat *et al* (1970), Spadaccini and Colket (1994)], but lower temperatures are of interest for ignition delay measurements of hydrocarbons [Ciezki and Adomeit (1993)], as shown in Fig. 4.

2d Rapid compression machines

In their most familiar role, rapid compression machines (RCM) comprise a mechanically driven piston which is used to compress a gaseous charge in a combustion chamber to a closed, constant volume following the end of compression. That is, there is no reciprocation as in a piston engine. The compression occurs sufficiently rapidly to induce heating of the gaseous charge, commonly in the range 500 - 1000 K according to the mechanical compression ratio and the ratio of heat capacities of the gaseous mixture. Very high pressures can easily be achieved (0.5 - 5 MPa) with a typical compression ratio of about 10:1. The charge is fuel + air, the fuel being either premixed as a vapour in oxygen and other diluting gases, or injected as liquid droplets.

The operating temperature range of the RCM is lower than that typical of shocked gas conditions and reaction times are several orders of magnitude greater than in shock tubes, $t < 100$ ms. These conditions also complement those of closed and flow reactors, especially with respect to the higher operating pressures and shorter reaction times in a rapid compression machine. Rapid compression machines are not without technical difficulty, nor are the data obtained easy to interpret quantitatively. Amongst the major technical problems associated with the operation of an RCM is the ability to attain a sufficiently fast compression, yet arrest the motion of the solid piston without vibration or bounce. The early development and applications of rapid compression machines have been reviewed by Jost [1949], Sokolik [1963] and Martinengo [1967]. The most prolific work output of ignition delay measurements subsequent to these dates has come from Shell, Thornton Research and Technology Centre [Fish et al (1969)], Leeds University [Griffiths *et al* (1993), (1997)] and Lille University [Minetti *et al* (1995)].

Amongst the main parameters of interest in rapid compression studies are the temperature and pressure that are reached at the end of compression. Pressure measurements are made by fast response pressure transducers (>10 kHz), and ignition delay times are measured from the pressure - time profiles (e.g. Figs 1 and 2). The measurements of pressure may be supplemented by the detection of light output through windows, and by chemical analysis at intermediate stages of reaction by rapid expansion and quenching methods [Fish *et al* (1969), Minetti *et al* (1995), Cox *et al* (1996)].

Although piston motion may be rapid, a perfect adiabatic compression does not always occur in an RCM. Heat losses to the chamber wall and boundary layer development as a result of the gas motion generated by the piston are the main causes of departures from ideality. Nevertheless, gas at the core of the compressed charge may be regarded to have experienced an adiabatic isentropic compression, assuming heat losses are confined to the boundary layer. In most, but not all circumstances, the core gas temperature, T_c, is the natural reference temperature for the compressed gas [Griffiths *et al* (1993)]. Because rates of heat loss are dependent on the combustion chamber geometry and the extent of gas movement created by the piston motion, the ignition delay for a given fuel mixture at a certain pressure will be apparatus dependent.

KINETIC BACKGROUND AND MECHANISMS OF OXIDATION

3a Introduction

As may be inferred from the temperature dependence of ignition delays for different classes of hydrocarbons (Section 1), there are significant qualitative and quantitative differences in their mechanisms of oxidation. The main distinctions exist between aromatic and aliphatic compounds, but these may become blurred if the aromatic structures also have aliphatic side chains. The purpose of this section is to give a perspective of the oxidation chemistry of the main classes of compounds, with also give some indications of their relative reactivities. The distinctions are drawn between alkanes, alkenes, cyclic alkanes (naphthenes) and aromatics. Whilst, for illustrative purposes, specific examples are used, the descriptions are intended to be interpreted in a general way, with relevance to fuels that fall in the normal boiling point range 350 - 550 K.

Most is known about the chemistry of alkane oxidation, especially where the components of gasoline (C_4 - C_{10}) are concerned. However, in this context there is a need to know as much about the oxidation chemistry of the more volatile aromatics (e.g. toluene) and about oxygenated fuels, such as the ethers (e.g. methyl t-butyl ether), since these also are significant components of unleaded gasoline. In some circumstances it is possible to infer aspects of the behaviour of one class from the detailed understanding of another, and this may be important as part of establishing an overview.

The temperature range of greatest interest for spontaneous initiation of ignition extends from about 750 K to 1500 K. Normally combustion is fully developed at higher temperatures and, if it is possible for the starting conditions to approach 1500 K there would be no difficulty of ignition with exceedingly short ignition delays. As has been illustrated in Section 1, some hydrocarbons and other classes of organic compounds can be sufficiently reactive to undergo ignition at temperatures lower than 750 K, and even at these temperatures at high pressures the ignition delays can be very short (< 10 ms). The mechanisms which lead to ignition from very low temperatures may be relevant to potential routes for the enhancement of ignition in less reactive fuels.

Before embarking on an appraisal of the mechanisms involved during the oxidation of different types of compounds, it is important to establish some of the kinetic features that determine reaction rates and mechanisms. Without exception, gas phase combustion is driven by free radical chain propagation. Several modes of chain branching, which are operative in different temperature regimes, are possible and these are very important. The nature of chain branching processes will be described where they emerge in the mechanistic discussion.

Changes of both pressure and temperature will have an effect, the latter normally being the most influential. There are major differences in chemistry which may be distinguished broadly below and above 1000 K, and it is most convenient to discuss reaction mechanisms with this division in mind. The distinction is brought about as a result of the relative rates of various types of elementary reactions and their temperature dependences, in the following way. Many of the kinetic parameters

given in the following sections are taken from Baulch *et al* [1992] and from Walker and Morley [1997].

Relative rates of chain initiation from the primary fuel

The spontaneous initiation of reaction may occur homogeneously either by decomposition of the primary fuel or by its reaction with oxygen. The activation energies involved are very high ($E > 200$ kJ mol^{-1}). Since decomposition implies a break-up of the carbon structure, whereas oxidation causes the structure to be retained in the first instance, the mechanism of the overall reaction may be pre-ordained to some extent by the predominant process, which is itself governed by the prevailing temperature. For example, with reference to dodecane (which may be regarded as a typical component of kerosene), the two possible reactions are

$C_{12}H_{26} \rightarrow C_6H_{13} + C_6H_{13}$, $k_1 = 4.0 \times 10^{16} e^{(-44743/T)}$ s^{-1}, (pyrolysis or degradation) (1)
alkane lower alkyl radical

$C_{12}H_{26} + O_2 \rightarrow C_{12}H_{25} + HO_2$, $k_2 = 1.8 \times 10^{14} e^{(-25000/T)}$ mol^{-1} cm^3 s^{-1}, (oxidation) (2)
alkane alkyl radical hydroperoxy radical

Their relative rates are given by

$$v_1/v_2 = k_1 / k_2 [O_2] \quad (3)$$

and exemplified in Table 1, when oxygen is assumed to be at its normal concentration in air at 1 bar and at the prevailing temperature.

Table 1. Relative rates of decomposition and oxidation of dodecane

T / K	750	1000	1250	1500
$(k_1/k_2)/mol^{-1}$ cm^3	8.21×10^{-10}	5.92×10^{-7}	3.07×10^{-5}	4.28×10^{-4}
v_1/v_{10}	3.16×10^{-4}	0.23	11.8	165

Only at temperatures well in excess of 1000 K is the degradation of the primary fuel molecule the predominant mode of initiation at normal oxygen concentrations. Both of these processes are highly endothermic. Neither the reaction rate parameters nor the endothermicity of the two specified types of reactions differ very greatly across the range of normal components of hydrocarbon fuels (Tables 2 and 3 [Walker and Morley (1997)]). However, the rates of oxidation of other compounds, such as aldehydes, are believed to be faster than those of hydrocarbons, because they present a very labile, acyl H atom for abstraction [Walker and Morley (1998)]. The activation energies in this case are about 150 kJ mol^{-1}, which is lower than the activation energies even for the most reactive initiation steps for hydrocarbons ($E >$ 160 kJ mol^{-1} in the case of propene and $E \sim 170$ kJ mol^{-1} in the case of toluene).

Table 2. Endothermicity for the reaction RH + O_2

The group from which H atom abstraction occurs is underlined

Reactant	ΔH^{O}_{298} / kJ mol^{-1}
C_2H_4	239
C_2H_6	213
$CH_3\ \underline{CH_2}\ CH_3$	200
$(CH_3)_3\ \underline{CH}$	190
$\underline{CH_3}\ CH{=}CH_2$	165
$(CH_3)_2\ C{=}CH\ \underline{CH_3}$	158
$(CH_3)_2\ C{=}C(CH_3)_2$	143
$CH_2{=}CH\underline{CH}CH{=}CH_2$	122
CH_2O	166
$C_2H_5\ CHO$	156
C_6H_6	254
$C_6H_5\ \underline{CH_3}$	169

Table 3. Arrhenius parameters for initiation by pyrolysis of C-C bonds

Reaction	log (A / s^{-1})	E / kJ mol^{-1}
Aliphatic hydrocarbons		
$C_2H_6 \rightarrow 2CH_3$	16.7	372
$C_4H_{10} \rightarrow 2C_2H_5$	16.5	343
$(CH_3)_2\ CHCH(CH_3)_2 \rightarrow 2(CH_3)_2\ CH$	16.4	319
$(CH_3)_3\ CCH(CH_3)_2 \rightarrow (CH_3)_2\ CH + (CH_3)_3C$	16.5	305
$(CH_3)_3\ CC(CH_3)_3 \rightarrow 2(CH_3)_3C$	16.8	290
$CH_2{=}CHCH_2CH_2CH{=}CH_2 \rightarrow 2\ CH_2{=}CHCH_2$	15.1	241
Aromatic hydrocarbons		
$^{*}C_6H_5\ CH_3 \rightarrow C_6H_5CH_2 + H$	15.5	373
$C_6H_5\ CH_2CH_3 \rightarrow C_6H_5CH_2 + CH_3$	15.6	306

*pyrolysis of the C-H bond

Relative rates of oxidation and degradation of the primary fuel

The propagation reactions are the principal means of reactant consumption by, for example

$$RH + OH \rightarrow R + H_2O \qquad (4)$$

where R would represent an alkyl radical generated from an alkane. Propagation by OH radicals is common throughout the whole temperature range, and it occurs with very low activation energy. For alkanes the rate constants may be classified with respect to each type of C-H bond (Table 4)

Table 4. Kinetic parameters for H atom abstraction by OH from alkanes

Type of abstraction	k / cm^3 mol^{-1} s^{-1}
primary C-H (k_p)	$2.7 \times 10^6 T^2 e^{-303/T}$
secondary C-H (k_s)	$2.6 \times 10^6 T^2 e^{233/T}$
tertiary C-H (k_t)	$1.1 \times 10^6 T^2 e^{710/T}$

where the subscripts p, s and t signify abstraction from a primary, secondary or tertiary site. Notice that a three parameter fit ($k = A T^n e^{-E/RT}$) is used to represent the rate constant over a very wide range of temperature. Also the temperature coefficient in the exponential term is expressed as (E/R) / K, and that it takes a negative value in two out of the three cases. In this expression, R is the gas constant.

Whether or not species R decomposes or oxidises depends upon the temperature and the concentration of oxygen. For example, the dodecyl radical may undergo the competitive reactions

$$\underset{\text{alkyl radical}}{C_{12}H_{25}} \rightarrow \underset{\text{alkene}}{C_6H_{12}} + \underset{\text{lower alkyl radical}}{C_6H_{13}}, \qquad k_5 = 2.5 \times 10^{13} e^{(-14433/T)} \ s^{-1} \qquad (5)$$

$$\underset{\text{alkyl radical}}{C_{12}H_{25}} + O_2 \rightarrow \underset{\text{alkene}}{C_{12}H_{24}} + \underset{\text{hydroperoxy radical}}{HO_2}, \qquad k_6 = 1.0 \times 10^{12} e^{(-1000/T)} \ mol^{-1} \ cm^3 \ s^{-1} \qquad (6)$$

and the relative rates are given by

$$v_5/v_6 = k_5 / k_6 \, [O_2] \qquad (7)$$

The relative magnitudes of the rate constants and the relative reaction rates at an oxygen molar density of 2.6×10^{-6} mol cm^{-3} (typical of atmospheric conditions), over the temperature range 750 - 1500 K, are given in Table 5.

Table 5. Relative rates of decomposition and oxidation of dodecyl radicals

T / K	750	1000	1250	1500
(k_5/k_6) /mol^{-1} cm^3	4.75×10^{-7}	4.05×10^{-5}	5.83×10^{-4}	3.45×10^{-3}
v_5/v_6	0.18	15.58	224	1327

The relative rates of reactions (5) and (6) are also susceptible to the prevailing oxygen concentration, such that decomposition would be favoured in very fuel rich conditions, but the predominance of oxidation would be maintained to a higher temperature during combustion at reaction pressures above ambient, even with air as the oxidising medium. Typical rate parameters for degradation of alkyl radicals are given in Table 6.

Table 6. Activation energies for pyrolysis of alkyl radicals (assuming A = 6.3 x 10^{13} s^{-1})

Reaction		E / kJ mol^{-1}
$(CH_3)_3CC(CH_3)_2 \rightarrow (CH_3)_2C{=}C(CH_3)_2 + CH_3$		158 ± 7
$(CH_3)_3CCH_2 \rightarrow (CH_3)_2C{=}CH_2 + CH_3$		148 ± 7
$(CH_3)_3CC(CH_3)_2\,CH_2 \rightarrow (CH_3)_3CC(CH_3){=}CH_2 + CH_3$		140 ± 7
$(CH_3)_3CCH(CH_3)\,CH_2 \rightarrow (CH_3)_3CCH{=}CH_2 + CH_3$		130 ± 7
$CH_3CH_2CHCH_2\,CH_3 \rightarrow CH_3CH_2CH{=}CH_2 + CH_3$		124 ± 7
$CH_3CHCH_2CH_2\,CH_3 \rightarrow C_3H_6 + CH_3$		122 ± 7
$(CH_3)_2C(CH)_2CH(CH_3)_2 \rightarrow CH_2{=}\,C(CH_3)CH(CH_3)_2 + CH_3$		121 ± 7
$(CH_3)_3\,CCH(CH_3)CH_2 \rightarrow t\text{-}C_4H_9 + C_3H_6$		111 ± 7
$(CH_3)_3CC(CH_3)_2\,CH_2 \rightarrow (CH_3)_3CC(CH_3){=}CH_2 + CH_3$		108 ± 7
$(CH_3)_2C(CH_2)CH(CH_3)_2 \rightarrow (CH_3)_2C{=}CH_2 + i\text{-}C_3H_7$		107 ± 7
lower alkyl radicals	A / s^{-1}	
$n\text{-}C_3H_7 \rightarrow C_2H_4 + CH_3$	1.6 x 10^{14}	136 ± 2
$n\text{-}C_4H_9 \rightarrow C_2H_4 + C_2H_5$	2.5 x 10^{13}	120 ± 4
$s\text{-}C_4H_9 \rightarrow C_3H_6 + CH_3$	2.3 x 10^{14}	137 ± 5
$i\text{-}C_4H_9 \rightarrow C_3H_6 + CH_3$	6.3 x 10^{13}	128 ± 7

Summary

The significance of these results is that there is an increasing tendency for the carbon structure of the fuel to be degraded as the temperature increases. Consequently, the chemistry at temperatures below 1000 K tends to be specific to the primary fuel structure, whereas at higher temperatures the reactions which take place are common to a very wide range of fuel molecules. In fact, since a species such as the hexyl radical shown as a product of reactions (1) and (5) is capable of decomposing in a similar way, as also will its further products, the overall chemistry at high temperatures is characteristic of that of much lower molecular mass species than the primary fuel. As illustrated by their formation in (1) and (5), an understanding of the mechanisms of combustion of alkenes is also relevant to a comprehensive picture of the combustion of alkanes, especially at higher temperatures.

3b The oxidation of alkanes at T < 1000 K

Alkylperoxy radical isomerisation

A generalised form of the underlying mechanism of oxidation of alkanes is given in Figure 14. The principal regimes relate to temperatures below about 800 K on the right hand side, and temperatures in the range from about 800 K to 1000 K on the left hand side. As is commonly accepted, R and R' refer to alkyl groups and Q refers to the fragment from an internal transfer of a hydrogen atom, often resulting in the formation of a partially oxygenated molecular intermediate (described as an O-heterocycle in Fig. 14) and an OH radical. For example, the production of 2,2,4,4-tetramethyltetrahydrofuran as a major product of i-octane oxidation results from the alkylperoxy radical isomerisation,

$$RO_2 \rightleftharpoons Q(1,6)OOH \qquad (8)$$

This involves either,

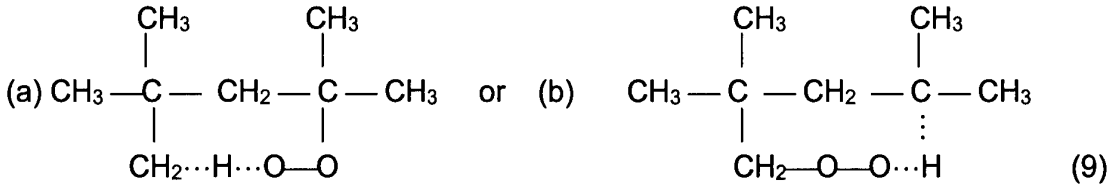

(9)

which is then followed either by decomposition initiated at the peroxide bond or by further addition of oxygen (Fig, 14). The distinction between these two forms shown in (9) can be made by the notation

$$(a)\quad R_tO_2 \rightleftharpoons Q(1,6p)OOH \qquad (10)$$

$$(b)\quad R_pO_2 \rightleftharpoons Q(1,6t)OOH \qquad (11)$$

in which the subscript t and p indicate that the transition occurs from a tertiary or a primary carbon atom site. A transition from a secondary site may be possible in other circumstances and would be signified as R_sO_2. The inclusion of (1.6p) or (1.6t) in QOOH indicates the size of the ring in the transition state, given by the transfer of H from a carbon atom, numbered as 1, to the second oxygen of the peroxy link, numbered as 6, and the nature of the site from which the H atom is transferred. All of these features are important because they will govern the activation energy associated with this type of rearrangement (Table 7) and, consequently, the relative reactivities of different alkanes or their isomeric structures in the low temperature range.

Table 7. Arrhenius parameters for alkylperoxy radical isomerisation reactions

Reaction	Type	10^{-12}A / s^{-1} (per C-H)	E/kJ mol^{-1}
$CH_3CH_2O_2 \rightarrow CH_2CH_2O_2H$	$R_pO_2 \rightarrow Q(1,4p)OOH$	1.41	154
$CH_3CH(O_2)CH_2CH_3 \rightarrow CH_2CH(O_2H)CH_2CH_3$	$R_sO_2 \rightarrow Q(1,4p)OOH$	1.41	155
$(CH_3)_3CCH_2O_2 \rightarrow CH_2CH(CH_3)_2CH_2O_2H$	$R_pO_2 \rightarrow Q(1,5p)OOH$	0.176	123
$(CH_3)_2CHCH_2O_2 \rightarrow CH_2CH(CH_3)CH_2O_2H$	$R_pO_2 \rightarrow Q(1,5p)OOH$	0.176	125
$CH_3(CH_2)_2CH_2O_2 \rightarrow CH_2(CH_2)_3O_2H$	$R_pO_2 \rightarrow Q(1,6p)OOH$	0.022	105
$CH_3(CH_2)_3CH_2O_2 \rightarrow CH_2(CH_2)_4O_2H$	$R_pO_2 \rightarrow Q(1,7p)OOH$	0.00275	105
$CH_3CH(O_2)CH_2CH_3 \rightarrow CH_3CH(O_2H)CHCH_3$	$R_sO_2 \rightarrow Q(1,4s)OOH$	1.41	138
$CH_3CH(O_2)(CH_2)_2CH_3 \rightarrow CH_3CH(O_2H)CHCH_2CH_3$	$R_sO_2 \rightarrow Q(1,4s)OOH$	1.41	133
$CH_3CH(O_2)(CH_2)_2CH_3 \rightarrow CH_3CH(O_2H)CH_2CHCH_3$	$R_sO_2 \rightarrow Q(1,5s)OOH$	0.176	109
$CH_3(CH_2)_3CH_2O_2 \rightarrow CH_3CH(CH_2)_3O_2H$	$R_pO_2 \rightarrow Q(1,6s)OOH$	0.022	91
$(CH_2)_3CHCH_2O_2 \rightarrow (CH_2)_3CCH_2O_2H$	$R_pO_2 \rightarrow Q(1,4t)OOH$	1.41	118

The role of dihydroperoxy species in promoting chain branching

The significance of the last remarks resides in the chain branching character of the low temperature combustion regime. The further addition of molecular oxygen

to the alkylhydroperoxy radical (QOOH) is known to yield alkylketohydroperoxides [Sahetchian *et al* (1991)], for example during n-heptane oxidation *via*

$$CH_3CH_2CH(OOH)CH_2CH_2CH(OO\cdot)CH_3 \rightleftharpoons CH_3CH_2C\cdot(OOH)CH_2CH_2CH(OOH)CH_3$$
$$\rightleftharpoons CH_3CH_2C(O)CH_2CH_2CH(OOH)CH_3 + OH \quad (12)$$

The molecular hydroperoxide is capable of undergoing further decomposition to form free radicals but, in addition, similar rearrangements may occur involving an H atom other than that at the hydroperoxy site. In these circumstances the product is not a molecular species, but a free radical.

$$CH_3CH_2CH(OOH)CH_2CH_2CH(OO\cdot)CH_3 \rightleftharpoons \quad (13)$$
$$CH_3CH_2CH(OOH)C(\cdot)HCH_2CH(OOH)CH_3$$

and its decomposition constitutes a branching reaction, such as

$$CH_3CH(OOH)C(\cdot)H(CH_2)_nCH(OOH)CH_3 \rightarrow 2CH_3CHO + C_2H_3 + 2OH \quad (14)$$

The combination of reactions (13) and (14) show that one radical generates three radicals, as is required in a chain branching process. Reaction (14) is likely to occur with an activation energy which is appreciably lower than that for molecular hydroperoxide decomposition. It will be close to that for with the decomposition of QOOH. The sequence of steps up to reaction (14) may satisfactorily account for the high reactivity of long chain n-alkanes at temperatures below 850 K.

By contrast, the reactivity of highly branched isomeric structures may be suppressed by alternatives to (14). For example the decomposition of the alkyldiperoxy species formed from neo-pentane may occur by

$$(CH_3)_2C(CH_2OOH)CH_2O_2\cdot \rightarrow CH_3COCH_3 + 2CH_2O + OH \quad (15)$$

This is a chain propagation process in which the reaction is continued via the OH radical.

Other low temperature branching modes

In Fig. 14 it is shown that branching can occur also by the decomposition of alkyl hydroperoxides, formed from an H atom abstraction reaction by RO_2, which circumvents the intervention of QOOH. There is also a contribution from hydrogen peroxide decomposition, displayed on the left hand side (T = 800 - 1000 K). The routes to the formation of each of these molecular species is via H atom abstraction reactions of RO_2 and HO_2 respectively. These radicals have to be amongst the predominant propagating species for there to be a significant rate of formation of the peroxides. As can be seen from Fig. 14, in general HO_2 formation is characteristic of the higher temperature region (T > 800 K). However, RO_2, is a product of the lower temperature range, and so the conditions at which each of the molecular peroxides is able to contribute to chain branching is quite markedly delineated. Moreover, the

activation energies for their respective decompositions are such that the alkyl hydroperoxide is able to contribute to chain branching (or degenerate chain branching, as it is called) at lower temperatures than the contribution from hydrogen peroxide (Table 8).

Table 8. Arrhenius parameters and half lives at 750 K for peroxide decompositions and secondary initiation by formaldehyde

Reaction	10^{-14}A / s^{-1} or $*mol^{-1}$ cm^3 s^{-1}	E/kJ mol^{-1}	$t_{1/2}$ / s at 750 K
$H_2O_2 \rightarrow 2OH$	3.2	197	0.11
$CH_3OOH \rightarrow CH_3O + OH$	40	179	5.0×10^{-4}
$CH_3(CH_2)_5OOH \rightarrow CH_3(CH_2)_5O + OH$	110	181	2.5×10^{-4}
$*CH_2O + O_2 \rightarrow HCO + HO_2$	2.0	163	244**

** O_2 at 3.2×10^{-6} mol cm^{-3}

On this basis, the simplest chain branching mechanism for low temperature alkane oxidation might be represented as

$RH + O_2$	$\rightarrow$	$R + HO_2$	initiation	(16)
$R + O_2$	$\rightarrow$	RO_2	propagation	(17)
$RO_2 + RH$	$\rightarrow$	RO_2H	propagation	(18)
RO_2H	$\rightarrow$	$RO + OH$	branching	(19)
$RO_2 + RO_2$	$\rightarrow$	molecular products	termination	(20)
$RO + RH$	$\rightarrow$	$ROH + R$	propagation	(21)
$OH + RH$	$\rightarrow$	$H_2O + R$	propagation	(22)

Whilst taking an idealised form, steps (16) - (22) demonstrate the foundation to an autocatalytic reaction, whereby the primary propagating species (R) is regenerated in an overall cycle (16 - 22) which gives the multiplication of radicals.

$R \rightarrow 3R$ (23)

It may appear also that the alkyl hydroperoxide route to chain branching should be the predominant low temperature mechanism, and early workers believed it to be so. However, the activation energies for H atom abstraction from the primary fuel by HO_2 or RO_2 are very high (Tables 9 and 10), which means that not only is the propagation slow, but also the RO_2 isomerisation may be the more favourable process. In fact, the isomerisation is potentially beneficial because aldehydes are amongst the partially oxygenated products of the isomerisation and QOOH decomposition. These have an exceedingly labile acyl H atom, which yields an activation energy for its abstraction by HO_2 or RO_2 ($E < 50$ kJ mol^{-1}) which is appreciably lower than that from the primary, secondary and tertiary sites of the alkanes (Tables 9 and 10). Thus aldehyde formation from QOOH can enable a faster route to the formation of alkyl hydroperoxides when

$RO_2 + R'CHO \rightarrow RO_2H + R'CO$ (24)

Table 9. Arrhenius parameters for HO_2 attack on alkanes (generic data)

Type of C-H	10^{-12}A / mol^{-1} cm^3 s^{-1} per C-H	E/kJ mol^{-1}
primary	1.9	85 ± 4
secondary	3.0	74 ± 4
tertiary	1.9	66 ± 4

Table 10. Arrhenius parameters for HO_2 attack on alkanes

Alkane	10^{-12}A / s^{-1} or *mol^{-1} cm^3 s^{-1}	E/kJ mol^{-1}
CH_4	8.9	103
C_2H_6	13.5	85 ± 3
$(CH_3)_3CC(CH_3)_3$	19.0	84 ± 6
c-C_6H_{12}	17.0	74 ± 5

Reactions of alkoxyl radicals

The mechanism represented by reactions (16) - (22) implies that H atom abstraction by alkoxyl radicals is there only fate. In fact, it is likely that they will either decompose to form an aldehyde or ketone together with an alkyl radical or H atom (Table 11), or react with molecular oxygen to form an aldehyde or ketone and an HO_2 radical (Table 11). These reactions will be of some relevance to the part played by additives to enhance the initiation rate (Section 4).

Table 11. Arrhenius parameters for alkoxyl radical decomposition and oxidation

Reaction	10^{-14}A / s^{-1} or *mol^{-1} cm^3 s^{-1}	E/kJ mol^{-1}
$CH_3O + M \rightarrow CH_2O + H + M$	*2.2×10^{17}	112
$C_2H_5O \rightarrow CH_2O + CH_3$	8.0×10^{13}	90
$(CH_3)_3CO \rightarrow (CH_3)_2CO + CH_3$	5.0×10^{13}	46
$CH_3O + O_2 \rightarrow CH_2O + HO_2$	*4.0×10^{10}	8.9
$C_2H_5O + O_2 \rightarrow CH_3CHO + HO_2$	*6.0×10^{10}	6.9
$(CH_3)_2CHO + O_2 \rightarrow (CH_3)_2CO + HO_2$	*9.0×10^{9}	1.7

The alkyl / alkylperoxy radical equilibrium

At the centre of Fig 14 is an equilibrium represented as

$$R + O_2 \rightleftharpoons RO_2 \qquad (25)$$

This part of the kinetic scheme plays a very important role in controlling the development of spontaneous ignition from low temperatures, and is a primary cause of two-stage ignition. Although dependent on the nature of the alkyl (or other) group, the equilibrium constants for this process are such that there is a marked

displacement from the formation of RO_2 to the predominance of R over the temperature range 650 - 850 K. This displacement is illustrated with respect to the temperature at which the equilibrium constant is equal to unity when oxygen is at its normal atmospheric concentration (Table 12).

Table 12. Data for the R + O_2 ⇌ RO_2 equilibrium

Radical	H	CH_3	C_2H_5	i-C_3H_7	t-C_4H_9	CH_2CHCH_2
ΔH^o_{298} / kJ mol^{-1}	-208	-135	-147	-155	-153	-75
log K / atm^{-1} (500 K)	16.8	7.4	7.6	7.7	7.1	1.6
log K / atm^{-1} (750 K)	9.6	2.7	2.45	2.25	1.75	-1.05
log K / atm^{-1} (1000 K)	6.0	0.35	-0.1	-0.45	-0.95	-2.35
log K / atm^{-1} (1250 K)	3.7	-1.15	-1.70	-2.1	-2.65	-3.15
T / K for [R] = [RO_2], [O2] = 0.2 atm	1920	930	900	860	820	550

Consequently, although exceedingly reactive channels which give OH radical production and chain branching occur at temperatures below 800 - 850 K via RO_2, as the temperature rises (as a result of the substantial heat release associated with OH propagation) there is an enforced displacement towards a largely non-branching reaction mode, which is dominated by HO_2 radical propagation, and from which relatively low heat release rates occur. Notably, an overall stoichiometry of the form

alkane + O_2 = alkene + H_2O_2 (26)

is virtually thermoneutral.

The effect of kinetic features such as these can be inferred from the form of the pressure - time profile shown in Fig. 2. The late development of the first stage is accompanied by a weak maximum in chemiluminescence, signifying that the free radical concentrations rise to a maximum and then decay. This is associated with the late stage of development of the low temperature chain branching. However, the accompanying temperature rise forces the reaction rate (and heat release rate) to slow down because the shift of the balance of the R / RO_2 equilibrium causes the main reaction pathway to be displaced towards that characterised by the mainly non-branching processes shown on the right hand side of Fig. 14.

Reactions of methyl radicals

It is clear from the foregoing section that, in many respects, the behaviour of methyl radicals must be distinctly different from that of the higher alkyl radicals. In particular, neither the formation of a corresponding alkene nor the alkylperoxy radical isomerisation are possible. Nevertheless, there may be some similarity through the reactions

$CH_3 + O_2 \rightleftharpoons CH_3O_2$ $k_{27f} = 7.8 \times 10^8 T^{-1.2}$ mol^{-1} cm^3 s^{-1} (27)

$CH_3O_2 + RH \rightarrow CH_3OOH + R$ (see Tables 9 and 10) (28)

Reaction (28) may involve organic intermediates other than alkanes, such as aldehydes (24), which enables a relatively active route to peroxide formation. Chain branching would follow through the decomposition of methyl hydroperoxide (see Table 8), but there is no scope for chain branching *via* diperoxy species. An alternative route to methylhydroperoxide formation is *via*

$$CH_3O_2 + HO_2 \rightarrow CH_3OOH + O_2 \qquad (29)$$

but this does not lead to chain branching as such, although it would lead to the formation of OH radicals as a propagating species.

An important supplementary reaction of CH_3 with oxygen is

$$CH_3 + O_2 \rightarrow CH_2O + OH \qquad k = 3.3 \times 10^{11} e^{-4500/T}\ mol^{-1}\ cm^3\ s^{-1} \quad (30a)$$
$$\rightarrow CH_3O + O \qquad k = 1.3 \times 10^{14} e^{-15830/T}\ mol^{-1}\ cm^3\ s^{-1} \quad (30b)$$

and the kinetic data for the lower activation energy branch indicate that it would compete successfully with the association step in (27), even at very low temperatures. However, the rate parameters for reaction (30a) are quoted over the temperature range 1000 - 2500 K [Baulch *et al* (1992)], so it is not clear how this competition should be interpreted in the lower temperature range. The activation energy for (30b) is too high for it to be at all influential at T < 1000 K.

3c The oxidation of alkenes at T < 1000 K

Much of the foregoing discussion about alkanes is applicable also to the aliphatic alkenes, especially for higher molecular mass compounds in which part of the carbon backbone is not disrupted by unsaturated links. Special features have to be addressed because alkenes are major intermediate products of alkane oxidation throughout the low temperature range. The reactivity of low molecular mass alkenes ($C_n < 6$) is of interest as well as that of alkenes that may be found as primary fuels in kerosene and related aviation fuels. There are three main sources, as follows.
(i) The lower molecular mass alkenes can be formed as products of QOOH decomposition.
(ii) Alkenes that are conjugate products of the primary alkane are formed as a result of displacement of the R /RO2 equilibrium towards dissociation (26).
(iii) The degradation of alkyl radicals also generates alkenes (5).

The distinction of the reactivity of alkenes is its susceptibility to free radical addition by H, OH, HO_2 and RO_2 to the double bond at temperatures below 1000 K. O atom addition is also favoured at higher temperatures. The generic representation of this addition process is

$$R'{-}CH{=}CH_2 + X \rightarrow R'{-}\dot{C}H{-}CH_2X \quad \text{or} \quad R'{-}CHX{-}\dot{C}H_2 \qquad (31)$$

H atom abstraction is also possible. If this occurs at a position which is remote from the double bond, the ensuing chemistry follows the patterns of behaviour that are similar to those of the alkanes. However, if abstraction takes place at a β position with respect to the double bond, electron delocalisation occurs

within the product alkenyl structure. This particular type of abstraction is favoured because the C-H bond on the β position is appreciably weaker than the normal bond strength associated with CH_2. That is, the activation energy for abstraction from a C-H at the β position is 52 kJ mol^{-1} versus 88 kJ mol^{-1}at other secondary C-H sites.

The delocalised electronic structure gives an enhanced stability (referred to as "resonance stabilisation"), and hence much reduced reactivity, to the radical product. This is exemplified by the exceedingly unreactive nature of propene (C_3H_6) at low temperatures as a result of the formation of the allyl radical (32). Allyl radical formation may pose problems if propene is formed as a molecular intermediate during combustion of higher molecular mass fuels at temperatures around 800 K.

$$CH_3 - CH = CH_2 + X \rightarrow \underset{\cdots\cdots\cdots\cdots}{CH_2 - CH - CH_2} + HX \qquad (32)$$

An important reaction in propene chemistry at low temperatures is the radical addition reaction between allyl and hydroperoxy radicals

$$CH_2 - CH - CH_2^{\cdot} + HO_2 \rightarrow CH_2 = CH - CH_2OOH \qquad (33)$$

This would be followed by decomposition of the peroxide linkage and further oxidation to form acrolein (CH_2CHCHO), and also formaldehyde (CH_2O) and formyl radicals (HCO), *via* C_2H_3, as shown below (36). At higher temperatures the reaction of OH with propene will be dominated by addition to the double bond, rather than the β H-atom abstraction type of process shown in (31) [Walker and Morley (1997)].

Ethene (C_2H_4) is not very reactive at temperatures below about 800 K. It is susceptible to radical addition at the double bond, although the activation energy for HO_2 addition, with the subsequent formation of an oxiran, is very high.

$$C_2H_4 + HO_2 \rightarrow C_2H_4OOH \rightarrow CH_2(O)CH_2 + OH \qquad E = 72 \pm 5 \text{ kJ mol}^{-1} \qquad (34)$$

Hydroxyl radicals are most likely to abstract an H atom from ethene by

$$C_2H_4 + OH \rightarrow > C_2H_3 + H_2O \qquad E = 25 \text{ kJ mol}^{-1} \qquad (35)$$

Oxidation of C_2H_3 is believed to lead to formaldehyde and the formyl radical by addition of molecular oxygen across the double bond.

$$C_2H_3 + O_2 \rightarrow CH(OO)CH_2 \rightarrow CH_2O + HCO \qquad (36)$$

The further oxidation of both of these species leads to the generation of HO_2 radicals as the main propagating species. At temperatures above 1000 K reaction of C_2H_2 with O atoms tends to cause the C-C bond to be split.

Oxidation of the straight chain butenes (1-butene and 2-butene, C_4H_8) appears to present special circumstances. H atom abstraction leads to the butenyl radical in either case, and its further reaction with oxygen occurs readily to form butadiene (C_4H_6) and HO_2 (37 and 38). This means that hydroperoxy radicals become the predominant propagating species in the low temperature region.

$$C_4H_8 + X \rightarrow \underset{\cdots\cdots\cdots\cdots\cdots\cdots}{CH_2 - CH - CH - CH_2} + HX \quad (37)$$

$$\underset{\cdots\cdots\cdots\cdots\cdots\cdots}{CH_2 - CH - CH - CH_2} + O_2 \rightarrow C_4H_6 + HO_2 \quad (38)$$

Moreover, chain propagation occurs mainly by

$$C_4H_8 + HO_2 \rightarrow C_4H_7 + H_2O_2 \quad (39)$$

and termination is mainly by

$$HO_2 + HO_2 \rightarrow H_2O_2 + O_2 \quad (40)$$

The decomposition of hydrogen peroxide will occur readily only at temperatures above about 900 K (see Table 8 and Section 3h) so the conversion from HO_2 to OH propagation is not very significant at lower temperatures. Note that, whereas hydrogen peroxide decomposition following reaction (39) is a chain branching process, it is not so when hydrogen peroxide is formed by hydroperoxy radical disproportionation (40). However, there is some possibility of branching reactions following the O_2QOOH route as a result of the addition reaction

$$C_4H_8 + HO_2 \rightarrow C_4H_8OOH \quad (41)$$

This type of reaction may be viable for butene but it is negligibly slow in propene oxidation [Stothard and Walker (1991)].

An overall perception is that the low molecular mass alkenes do not react readily at low temperatures, and certainly far less readily than the corresponding alkanes. There is a strong propensity for HO_2 formation, which then act as the primary (and slow) propagating species. If the lower alkenes are formed as intermediates during oxidation, they may tend to have a moderating (or retarding) influence on the overall reaction.

3d The oxidation of cycloalkanes (naphthenes) at T < 1000 K

Cyclohexane is representative of the class of compounds and it is probably the most studied of the cycloalkanes as far as chemical understanding is concerned [Zeelenberg and de Bruijn (1965), Griffiths *et al* (1968), Gulati and Walker (1989)]. There has also been some investigation of cyclopentane [Handford-Styring and Walker (1995)]. These compounds and their alkyl substituted analogues are present in significant proportions in gasoline. Both cyclopentane and cyclohexane are readily susceptible to H atom abstraction by H or OH (Table 13 [Baldwin and Walker (1981)]).

Table 13: Kinetic parameters for radical attack on cycloalkanes ($AT^ne^{(-E/RT)}$)

Reaction	A / mol^{-1} cm^3 s^{-1}	n	(E/R) / K	T / K
H + c-C_5H_{10}	2.4×10^9	1.5	2440	300 - 1200
H + c-C_6H_{12}	3.4×10^9	1.5	2440	300 - 1000
OH + c-C_5H_{10}	3.7×10^5	2.5	-519	300 - 1500
OH + c-C_6H_{12}	6.7×10^9	1.5	-125	300 - 1000

Cyclohexane undergoes spontaneous ignition readily from temperatures of 500 K in closed vessels [Snee and Griffiths (1989)], and two-stage ignition can be induced in a non-isothermal flow tube from about 600 K, with a cool flame development above 750 K and running into the second stage chemistry above 850 K [Griffiths *et al* (1968)]. At temperatures around 750 K the primary products of oxidation include o-heterocycles of cyclohexane and cyclohexene. However, hex-5-en-1-al is also a major primary product, which indicates that the ring is quite readily broken [Baldwin and Walker (1981)]. The non-planar structure of cyclohexane contributes through a moderation of the strain energy associated with the transition ring during isomerisation. A proposed mechanism involves peroxy radical isomerisation and decomposition is as follows

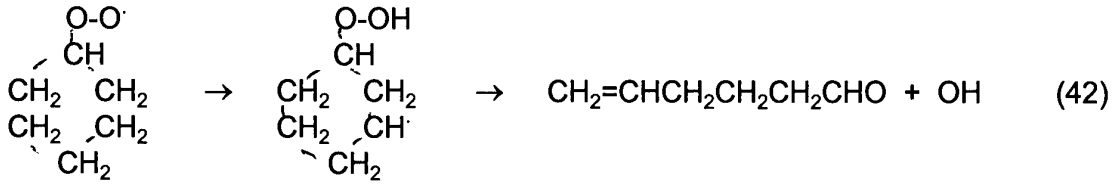

Whilst decomposition of the cyclohexyl radical may also occur to give ethene and the butenyl radical, i.e.

$$c\text{-}C_6H_{11} \rightleftharpoons CH_2{=}CHCH_2CH_2CH_2CH_2^{\cdot} \rightarrow C_2H_4 + CH_2{=}CHCH_2CH_2^{\cdot} \qquad (43)$$

leading to the formation of butadiene by H atom abstraction, this is favoured only at temperatures appreciably above 1000 K because the reverse of (43) occurs very readily at lower temperatures. A similar mode of decomposition of the cyclopentyl radical formed from cyclopentane to that shown in (43) is possible, but the decomposition route is more strongly favoured because there is a more substantial activation energy associated with the cyclisation of the pentenyl radical than that of the hexenyl radical.

Benzene can also be a product of the later stages of cyclohexane oxidation at temperatures below 1000 K, which occurs most probably by a sequence of H atom abstraction reactions consecutively by free radicals and molecular oxygen. The higher molecular mass, alkyl substituted naphthenes may undergo similar types of reactions to those described above.

3e The oxidation of aromatic compounds at T < 1000 K

The oxidation of the lowest molecular mass aromatic compounds (e.g. benzene and toluene) is rather different from that of the aliphatic structures, but some similarities can begin to emerge if aliphatic side-chains of two or more carbon atoms are substituted in the aromatic ring. At very low temperatures benzene is subject only to radical substitution reactions, the most notable being that of O atoms, by

$$C_6H_6 + O \rightarrow C_6H_5OH \text{ or } C_6H_5O + H^{\cdot} \qquad (44)$$

H atom abstraction is exceptionally difficult because the C-H bond strength is about 465 kJ mol^{-1}. The principal reactions of the substituted benzene involves reaction of

the side-chain, usually as an H atom abstraction. Toluene and ethyl benzene yield highly delocalised, and therefore very stable, radical structures, i.e.

$$C_6H_5CH_3 + X \rightarrow C_6H_5CH_2 + HX \quad (45)$$
$$C_6H_5C_2H_5 + X \rightarrow C_6H_5CHCH_3 + HX \quad (46)$$

It is believed that the R/RO_2 equilibrium for benzyl radicals

$$C_6H_5CH_2 + O_2 \rightleftharpoons C_6H_5CH_2O_2 \quad (47)$$

favours the benzyl radical [Fenter *et al* (1994)] from rather low temperatures. Even in circumstances which favour the formation of $C_6H_5CH_2O_2$ there is no opportunity for an intramolecular rearrangement of the kind that is possible in alkane oxidation. The most important types of reactants for the benzyl radical and similar derivatives of other aromatic compounds are likely to be the radical recombinations of the kind associated with allyl radicals. In particular, benzaldehyde is a product of the addition of HO_2 to the benzyl radical, followed by peroxide decomposition and H atom abstraction by O_2 [Baldwin *et al* (1986)].

$$C_6H_5CH_2 + HO_2 \rightarrow C_6H_5CH_2O_2H \rightarrow C_6H_5CH_2O + OH \quad (48)$$

A similar reaction is possible between the $C_6H_5CHCH_3$ radical, formed from ethyl benzene, and HO_2 to form benzaldehyde, but it has a chain branching character insofar that both OH and CH_3 are believed to be produced. The $C_6H_5CHCH_3$ radical is also able to react with oxygen to form styrene by H atom abstraction [Walker and Morley (1997)].

One important aspect of aromatic oxidation chemistry is how, or at what stage, the benzene ring is broken. The present understanding is that, at temperatures above 750 K, the oxidation of the phenyl radical is the precursor to decomposition, first to a cyclopentadienyl radical by elimination of CO then by its oxidation through reaction with HO_2.

The intermediate stage

$$C_6H_5O \rightarrow c\text{-}C_5H_5^{\cdot} + CO \quad (49)$$

is believed to have the rate constant $k = 2.5 \times 10^{11} e^{-22130/T}$. Ring opening is believed to occur after this stage, to form a C_4H_5 radical. The full sequence is as follows

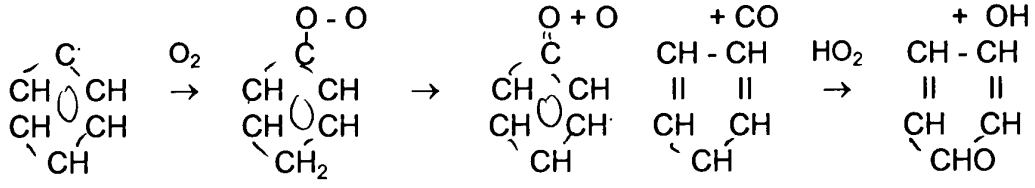

(50)

$$C_5H_5O \rightarrow CH_2{=}CHCH{=}CH^{\cdot} + CO \quad (51)$$

The intermediate formation of C_6H_5O and O is a chain branching process [Baldwin *et al* (1986)]. If toluene is susceptible to H atom abstraction from the aromatic ring by free radicals (such as HO_2) then an equivalent reaction is possible, i.e.

$$C_6H_5CH_3 + HO_2 \rightarrow C_6H_4CH_3 + H_2O_2 \quad (52)$$
$$C_6H_4CH_3 + O_2 \rightarrow C_6H_4(O^{\cdot})CH_3 + O \quad (53)$$

Rate constants for reactions of alkylbenzenes with simple radicals are summarised in Table 14.

Table 14. Kinetic parameters for radical / alkylbenzene reactions ($k = AT^n e^{-E/RT}$)

Reaction	$10^{-14}A$ / *mol^{-1} cm^3 s^{-1}	n	(E/R) / K
$O + C_6H_6 \rightarrow OH + C_6H_5 / C_6H_6O$	35.53	3.8	473
$O + C_6H_5CH_3 \rightarrow$ products	3.2×10^9	1.21	1200
$O + C_6H_5C_2H_5 \rightarrow$ products	1.7×10^{13}	0	1840
$O + p\text{-}C_6H_5(CH_3)_2 \rightarrow$ products	1.7×10^{13}	0	1630
$H + C_6H_5CH_3 \rightarrow C_6H_5CH_2 + H_2$	397.5	3.44	1570
$OH + C_6H_6 \rightarrow C_6H_5 + H_2O$	1.6×10^8	1.42	730
$OH + C_6H_6 \rightarrow C_6H_5OH + H$	1.3×10^{13}	0	5330
$OH + C_6H_5CH_3 \rightarrow C_6H_5CH_2 + H_2O$	5.2×10^9	1.0	440
$HO_2 + C_6H_5CH_3 \rightarrow C_6H_5CH_2 + H_2O_2$	4.0×10^{11}	0	780
$HO_2 + C_6H_5CH_3 \rightarrow C_6H_4CH_3 + H_2O_2$	5.5×10^{12}	0	14500

3f The oxidation of aromatic compounds at T > 1000 K

Continuity is most easily maintained by addressing the oxidation of aromatic compounds first in the high temperature regime (T > 1000 K). The most substantial experimental work has originated from Princeton University, from studies in the turbulent flow reactor at temperatures in the range 1000 - 1200 K [Emdee *et al* (1990, 1992)]. There are also shock tube studies that contribute to the understanding of the chemistry [Braun-Unkhoff *et al* (1989)]. The key to the main reaction path for benzene is that the equilibrium

$$C_6H_5 + O_2 \rightleftharpoons C_6H_5O_2^{\cdot} \quad (54)$$

is displaced in favour of C_6H_5 at temperatures above 1000 K. Consequently, the decomposition of C_6H_5 is the dominant reaction, in competition with radical - radical reactions. The decomposition leads to a variety of highly unsaturated species which, ultimately, favour soot formation in fuel rich conditions. Many aspects of the subsequent oxidation are also common to that of aliphatic compounds at temperatures above 1000 K.

$$C_6H_5 \rightarrow {}^{\cdot}CH{=}CHCH{=}CHC{\equiv}CH \quad (55)$$
$$C_6H_5 \rightarrow CH{\equiv}CCH{=}CHC{\equiv}CH + H \quad (56)$$
$$C_6H_5 \rightarrow C_2H_2 + {}^{\cdot}CH{=}CHC{\equiv}CH \quad (57)$$
$$C_6H_5 \rightarrow C_2H_3 + CH{\equiv}CC{=}CH^{\cdot} \quad (58)$$
$$C_6H_5 \rightarrow C_2H^{\cdot} + CH_2{=}CHC{\equiv}CH \quad (59)$$

3g The oxidation of alkanes and other aliphatic compounds at T > 1000 K

As discussed at the beginning of Section 3, the primary fuel and radicals derived from it readily decompose at temperatures in excess of 1000 K. This leads to common reaction mechanisms for the combustion of many hydrocarbons. The mechanisms are related to the oxidation of low molecular mass species, as shown in Fig. 15 [Warnatz (1984)]. C_1 and C_2 species are readily generated in pyrolysis and degradation processes, and the main routes to the final products of combustion follow from the oxidation of these species. There can also be the onset of soot formation by polymerisation in fuel rich conditions. An overview of the progress to complete oxidation of a hydrocarbon fuel molecule (RH) may be regarded to involve the sequence of molecular species

$$RH \rightarrow CH_2O \rightarrow CO \rightarrow CO_2. \qquad (60)$$

The main source of heat release during the combustion of hydrocarbons comes from the formation of the final products of combustion, CO_2 and H_2O, with significant contributions also from the recombination of propagating free radicals in termination processes. CO formation is also accompanied by heat release, and it may be a final product during inefficient combustion regimes, such as in very fuel rich conditions. Virtually all CO_2 is formed by the oxidation of CO, usually involving OH radicals

$$CO + OH \rightarrow CO_2 + H \qquad k_{61} = 6.3 \times 10^6\, T^{1.5}\, e^{(250/T)}\ mol^{-1}\ cm^3\ s^{-1} \qquad (61)$$

Thus the failure to achieve complete combustion to CO may arise because of competition for OH radicals by other organic species, e.g.

$$RH + OH \rightarrow R + H_2O \qquad \text{(see Table 4)} \qquad (62)$$

The main propagating species of the chain reactions at temperatures above 1000 K are H, O , OH, HO_2, R and RO, where R represents a fragment of a hydrocarbon fuel molecule (such as the alkyl radical). The role of H atoms is extremely important but can be restricted by the reaction conditions, as discussed in the next section.

The diagrammatic form of Fig. 15 [Warnatz (1984)] includes solid lines to represent single step reactions and broken lines to represent more complex sequences from one stage to the next. The inclusion of forward and backward reactions in some cases is not intended here as an indication of "chemical equilibrium", and does not imply that other sequences ar not allowed to proceed in either direction. Whether or not this occurs is a consequence of the temperature dependence of the elementary reactions involved. For example, one of the main termination reactions is the recombination

$$H + OH + M \rightleftharpoons H_2O + M$$

$$k_{63f} = 1.0 \times 10^{16}\, e^{(900/T)}\ cm^6\ mol^{-2}\ s^{-1} \qquad (63f)$$

$$k_{63r} = 1.0 \times 10^{17}\, e^{(-58650/T)}\ cm^3\ mol^{-1}\ s^{-1} \qquad (63r)$$

in which M plays the part of a "chaparone" species and represents any molecule in the system which is capable of contributing kinetic energy or taking up excess

energy. The equilibrium constant K_{65} takes the values given in Table 15 from these kinetic data, and it is given by

$$K_{63} = \frac{[H_2O]}{[H][OH]}$$

Table 15. Equilibrium constant for H + OH + M ⇌ H_2O + M

T / K	1000	2200	3000
K_{63} / mol^{-1} cm^3	1.2×10^{25}	2.5×10^{10}	2.3×10^{7}

Thus at low temperatures the forward reaction acts as an extremely effective radical sink, insofar that the recombination effectively locks up the propagating species as water. At much higher temperatures the equilibrium is displaced sufficiently far to the left hand side that the radical pool is maintained at a significant concentration (by a factor of 10^8 in this illustration). This arises from the ability of water to dissociate readily when the temperature is sufficiently high. Chain termination is then much less effective, such that high concentrations of radicals are kept in the system and many radical - radical interactions, which may have been reasonably disregarded at low temperatures, must be taken into account. For example, whereas for the reaction

$$CH_3 + O_2 \rightleftharpoons CH_3O + O \qquad (30b)$$

the forward reaction alone may be considered at temperatures near 1000 K, the reverse reaction must be taken into account at the temperatures associated with flames.

3h Chain branching at T > 1000 K

How reaction develops, and the time taken to ignition (the ignition delay), depends upon chain branching. Throughout much of the temperature range, the most important of the branching reactions is known to be

$$H + O_2 \rightarrow OH + O \qquad (64)$$

supplemented by

$$O + RH \rightarrow OH + R \qquad (65)$$

However, a competition with the branching reaction (64) occurs by the association reaction

$$H + O_2 + M \rightarrow HO_2 + M \qquad k_{66} = 2.3 \times 10^{18}\ T^{-0.8}\ mol^{-2}\ cm^6\ s^{-1} \qquad (66)$$

The relative reaction rates are given by

$$v_{64} / v_{66} = k_{64} / k_{66}[M]. \qquad (67)$$

Whether or not chain branching predominates is strongly dependent on temperature, as shown in Table 16, where the total species concentration, [M], is taken to be 1.22×10^{-5} mol^{-1} cm^3 (corresponding to air at 1 bar and 1000 K).

Table 16. Relative rates of branching and non-branching via H + O_2

T / K	750	1000	1250	1500
(k_{64}/k_{66}) /mol^{-1} cm^3	1.09×10^{-7}	2.33×10^{-6}	1.49×10^{-5}	5.3×10^{-5}
v_{64}/v_{66}	8.9×10^{-3}	0.19	1.22	4.34

According to the relative reaction rate under these condition, there is the potential for chain branching to become the predominant step in the combustion reaction, at atmospheric pressure, only at temperatures above about 1200 K. However, there is also an inverse dependence on the total concentration of species in the system, [M], such that chain branching becomes increasingly more difficult to achieve as the pressure is raised. The temperature dependence of $v_{64}/v_{66} = 1$ is shown as a function of pressure in Figure 16.

4. ENHANCEMENT OF INITIATION BY ADDITIVES

4a Introduction

The most effective mode of enhancement of ignition is generally thought to be achieved by the inclusion of compounds in the fuel that decompose readily to produce free radicals, which promote the initiation of reaction chains [Li and Simmons (1986)]. The choice of compounds is governed by the existence of exceptionally weak bonds in the structure (CO-N, in nitrates or nitrites and O-O in peroxides, for example), which permit appreciably lower activation energies for initiation than are normally encountered during hydrocarbon oxidation. The main area in which this technique has been exploited is to improve the performance of diesel fuels, but the mechanisms involved are still not well understood [Al-Rubaie *et al* (1992), Clothier *et al* (1993)]. There is a view also that thermal augmentation, as a result of the exothermic decomposition and subsequent reactions from the promoting additives, may make a significant contribution to the reduction of ignition delays [Inomata *et al* (1990)].

The most widely encountered compounds as initiators are organic peroxides and nitrates, but there are other compounds that may also be capable of performing this function. The addition of the oxygenated intermediates of alkane oxidation at low temperatures, such as aldehydes and ethers, have also been considered as a mode of enhancement of initiation through their further oxidation. The purpose of this section is to address the mechanisms of reaction of the types of compounds that are capable of performing as ignition enhancers of hydrocarbon fuels.

4b Decomposition of dialkyl peroxides and alkyl hydroperoxides

As shown in Table 8, alkyl hydroperoxides decompose readily at temperatures above 600 K, and there half lives can be extremely short. Equally reactive, but

generally more safe for bulk handling, are the dialkyl peroxides. Within this classification, the compound that has been studied most extensively is di-t-butyl peroxide. Its mechanism of decomposition and thermochemistry is as follows.

	k / s^{-1} or $*mol^{-1}$ cm^3 s^{-1}	ΔH°_{298} / kJ mol^{-1}	
$(CH_3)_3COOC(CH_3)_3 \rightarrow 2(CH_3)_3CO$	$2 \times 10^{15}\ e^{-18282/T}$	168	(68)
$(CH_3)_3CO \rightarrow (CH_3)_2CO + CH_3$	$5 \times 10^{13}\ e^{-5533/T}$	17.65	(69)
$CH_3 + CH_3 \rightarrow C_2H_6$	$*2.5 \times 10^{13}$	-371.2	(70)

The initial step (68) is rate determining and the reaction is overall modestly exothermic (ΔH°_{298} = - 170 kJ mol^{-1}). The reaction is not a chain reaction because the recombination of the methyl radicals (71) occurs more readily than the abstraction of H atoms by CH_3 from the primary C-H sites of the reactant. Nevertheless, the combination of a significant activation energy and the exothermicity for the decomposition mean that di-t-butyl peroxide is capable of undergoing thermal ignition [Griffiths and Singh (1982), Griffiths and Mullins (1984)].

In excess oxygen at temperatures up to about 800 K the reaction of di-t-butyl peroxide gives an overall stoichiometry of the form [Williams *et al* (1976), Griffiths and Phillips (1990)]

$$(CH_3)_3COOC(CH_3)_3 + 1.7O_2 = 2.0(CH_3)_3CO + 1.7CH_2O + 0.3CH_3OH + 0.7H_2O_2 \quad (71)$$

from which ΔH°_{298} = - 436 kJ mol^{-1}. The quantitative yield of dimethyl ketone, and the measured overall rate constant [Griffiths and Singh (1982)] indicate that the initiation (68) is still the rate determining step. The supplementary products, as well as the extra heat generated, arise from the oxidation of methyl radicals formed in (69). Acetone is not sufficiently reactive to undergo oxidation readily in this temperature range, and the activation energies for abstraction of H atoms from its primary C-H bonds are too high for there to be an effective propagation by this means. The reaction shows no sign of any chain-branching character [Griffiths and Mullins (1984)]. A brief kinetic scheme [Griffiths *et al* (1985)] and a more detailed mechanism [Griffiths and Phillips (1990), Griffiths *et al* (1993)] have been used to make numerical predictions of ignition of di-t-butyl peroxide involving oxygen. The half-life for the decomposition (and oxidation) of di-t-butyl peroxide at 500, 600 and 700 K is 2.62 s, 5.9 ms and 76 μs respectively. Many dialkyl peroxides will behave in a similar manner, and will decompose at similar rates.

The generation of methyl radicals, and CH_3O or CH_3O_2 which may follow from them, is not of great advantage because chain branching is not readily established when the only H atom abstraction reactions involve primary C-H groups. The decomposition of alkyl hydroperoxides differs to the extent that hydroxyl radicals are formed on homolysis of the O-O bond. These may facilitate a greater reactivity because of their highly reactive nature (Table 4). The potential effect, as well as the consequence of other organic compounds being present with the peroxides, are discussed later.

4c Decomposition of alkyl nitrates

Alkyl nitrates have been used to a limited extent in liquid form as rocket monopropellants, and other organic counterparts, as solids, are used extensively as

explosives and propellants. The potential role as initiators stems from the possibility of chain initiation by free radicals, enhanced oxidation by nitrogen oxides and the increase of temperature resulting from heat release. The way in which alkyl nitrates may behave can be illustrated with reference to the decomposition and oxidation of isopropyl nitrate.

The decomposition of isopropyl nitrate ($C_3H_7ONO_2$) occurs readily at temperatures above 600 K and an overall stoichiometry for reaction is given by Beeley *et al* (1980a) as

$$1.0C_3H_7ONO_2 = 1.0CH_3CHO + 0.4CH_2O + 0.3CH_3NO_2 + 0.1\ CH_3ONO + 0.1CH_3OH + 0.1CH_4 + 0.05CO + 0.05CO_2 + 0.1HNO_2 + 0.25N_2O + 0.15H_2O \quad (72)$$

from which ΔH^o_{298} = -110 kJ mol^{-1}. At temperatures around 1000 K the overall stoichiometry becomes

$$1.0C_3H_7ONO_2 = 1.0CH_3CHO + 0.4CH_2O + 0.3CH_3NO_2 + 0.1\ CH_3ONO + 0.1CH_3OH + 0.1CH_4 + 0.05CO + 0.05CO_2 + 0.1HNO_2 + 0.25N_2O + 0.15H_2O \quad (73)$$

from which ΔH^o_{298} = -130 kJ mol^{-1} [Beeley et al (1980a)]. At still higher temperatures, more heat is released (ΔH^o_{298} = -360 kJ mol^{-1}), according to the simplified stoichiometry [Griffiths *et al* (1976)]

$$1.0C_3H_7ONO_2 = 0.5CO_2 + 1.5CO + 1.0CH_4 + 1.0H_2 + 0.5H_2O + 0.5N_2 \quad (74)$$

Considerably more heat is generated if oxygen is present, and the overall stoichiometry is no longer strongly dependent on the initial temperature. The restricting factors are the extent to which CO is oxidised to CO_2 and fuel bound N is converted to N_2, but a typical stoichiometry is given by Beeley *et al* (1984) as

$$1.0C_3H_7ONO_2 + 2.9O_2 = 2.2CO_2 + 0.5CO + 0.3CH_2O + 3.2H_2O + 0.4N_2O + 0.1N_2 \quad (75)$$

from which ΔH^o_{298} = -1500 kJ mol^{-1}.

These reactions are difficult to interpret as a kinetic mechanism, but there are a number of clear features [Beeley *et al* (1980b)]. First, even in the presence of oxygen, the overall rate is governed by the decomposition of isopropyl nitrate according to the following types of reactions

$$C_3H_7ONO_2 \rightarrow (CH_3)_2CHO + NO_2 \quad (76)$$
$$(CH_3)_2CHO \rightarrow CH_3CHO + CH_3 \quad (77)$$
$$CH_3 + NO_2 \rightarrow CH_3O + NO \quad (78)$$
$$CH_3 + NO_2 \rightarrow CH_3NO_2 \quad (79)$$
$$CH_3O + NO_2 \rightarrow CH_2O + HONO \quad (80)$$
$$HONO + M \rightarrow OH + NO \quad (81)$$

The nitrogen oxides play a powerful oxidising role, and they may contribute to the further oxidation of the intermediate aldehydes CH_3CHO and CH_2O [Pedler and Pollard (1957)]. Supplementary oxidation of the intermediate aldehydes and methyl radicals (27 - 30) also occurs by molecular oxygen, which may increase the free

radical pool in the late stages of reaction. This does not constitute chain branching with respect to the primary reactant because the isopropyl nitrate decomposes independently of this and is not subject to free radical attack. However, there may be a relevance of the build up of a radical pool in the context of the sensitisation of ignition of other hydrocarbon fuels by isopropyl (or other) alkyl nitrates. The same may be true of the involvement of the oxides of nitrogen (see below).

There are indications that a synergism may exist between different classifications of additives, as shown by the enhanced reduction of ignition delay of diesel fuels when isopropyl nitrate is mixed with di-t-butyl peroxide compared with that arising from the same total proportion of di-t-butyl peroxide alone [Al-Rubaie *et al* (1991)]. Quite complex nitrates have been used for enhancing the performance of diesel fuel, such as 2-ethyl hexyl nitrate, the rate constant for decomposition of which is given by $k = 2.5 \times 10^{15} e^{-18854/T} s^{-1}$ [Pritchard (1989)]. This gives half lives which fall from 12 ms to 22 μs when the temperature is raised from 600 to 750 K.

4d Oxidation of reactive molecular intermediates

Aldehydes and ethers are noted for their considerably greater reactivity than hydrocarbons. For example, acetaldehyde (ethanal) gives rise to cool flames and spontaneous ignition at temperatures below 500 K, and both diethyl ether and diisopropyl ether show similar modes of reactivity at still lower temperatures [Griffiths and Scott (1987)]. An overall stoichiometry for the oxidation of acetaldehyde below 600 K was given by Gray *et al* (1981) as

$$1.0CH_3CHO + 0.95O_2 = + 0.25CH_2O + 0.5CH_3OH + 0.1CH_4 + 0.8CO + 0.4CO_2 + 0.55H_2O \quad -370 \text{ kJ mol}^{-1} \qquad (82)$$

The reactivity stems from the ease with which chain branching can occur, as may be illustrated by the following simplified kinetic mechanism. Detailed numerical analyses giving a quantitative simulation of the combustion of acetaldehyde are reported elsewhere [Griffiths and Sykes (1989)].

$RCHO + O_2$	$\rightarrow >$	$RCO + HO_2$	initiation	(83)
$RCO + O_2$	$\rightleftharpoons$	RCO_3	propagation	(84)
$RCO_3 + RCHO$	$\rightarrow$	RCO_3H	propagation	(85)
RCO_3H	$\rightarrow$	$R + CO_2 + OH$	branching	(86)
$RCO_3 + RCO_3$	$\rightarrow$	molecular products	termination	(87)
RCO	$\rightarrow$	$R + CO$	propagation	(88)
$R + O_2$	$\rightleftharpoons$	RO_2	propagation	(25)

This structure has much in common with that set out for the alkanes, in reactions (16) - (22), and there is a supplementary mechanism of oxidation that follows the pattern for the alkanes once the species R is generated, as shown in (86) and (25). The quantitative difference between the reactivities of alkanes and aldehydes or

ethers (which readily lead to aldehydes and alkoxyl radicals during their low temperature oxidation) arises from the extremely labile H atom which is associated with the acyl group. This means that activation energies for propagation are unusually low and, in addition, the decomposition of the peracid intermediate (86) is exceptionally rapid.

The argument in favour of adding such compounds as sensitisers is that, since they are considerably more reactive than a primary hydrocarbon fuel, and aldehydes are molecular intermediates of the low temperature oxidation regime, the induction time to ignition can be reduced considerably by adding suitable quantities of such intermediates to the fuel mixture.

4e Reactivity of additives in hydrocarbon fuels

The mechanisms for reaction of different classes of compounds that are described in the preceding subsections concern their behaviour as the primary reactant. Significant differences must arise when these types of compounds are added to a hydrocarbon fuel. The most satisfactory way of investigating how the system might then behave is through numerical simulation, and this is discussed below. However, it is appropriate also to consider the qualitative implications for the role of additives.

Each of the systems considered above constitutes a source of free radicals, which may be generated exceedingly rapidly when the peroxides or nitrates decompose even at temperatures below 700 K. In neither of these cases, even in the presence of oxygen, is a chain reaction able to develop. However, in the presence of other hydrocarbon fuel molecules, chain reaction may be initiated by H atom abstraction. This then constitutes an accelerated generation of the primary reaction chains for oxidation of the fuel.

The promotion of the combustion of 1-octene by di-t-butyl peroxide and by isopropyl nitrate is illustrated in Figs 12 and 13. The "baseline" flow-tube temperature was 685 +/- 10 K in these experiments (see section 2b), so the highest temperature reached during reaction was no more than 750 K. Even with the moderating influence on the reactant temperature brought about by the liquid fuel vaporisation, both the peroxide and the nitrate will have decomposed within several centimetres after injection. The maximum temperature increase was, almost certainly, set by the onset of the negative temperature dependence of reaction rate in that temperature range. Reactant depletion would account for the subsequent decrease in ΔT. The fuel concentration was not measured directly in these experiments. Whilst a quantitative basis for the interpretation of the effectiveness of the additive from these experiments has yet to be devised, it is clear that increased amounts of each of the additive enhances the reactivity. There is no significant distinction between the performance of either the di-t-butyl peroxide or the isopropyl nitrate. However, the slightly higher temperatures that are achieved by the system including isopropyl nitrate might be construed as a consequence of reactions of molecular intermediates promoted by the nitrogen oxides.

Just how effective the process is depends upon relative reactivities of the radical with respect to the fuel. Hydroxyl radicals are certainly the most favourable

species because their abstraction is unselective (Table 4). HO_2 or RO_2 are amongst the least desirable initiating radicals because the activation energies for H atom abstraction are very high (Tables 9 and 10), and a limitation on their effectiveness is that radical recombination may have a higher probability (e.g. reaction (29)).

There is, however, a fundamental constraint on the effectiveness of any free-radical enhancement of hydrocarbon ignition when the initiators decompose very readily at low temperatures. This can be inferred from Figs. 2 and 3. The development of spontaneous ignition of the aliphatic hydrocarbons follows a two-stage pattern. If an additive readily generates free radicals at temperatures in the range 600 - 750 K, then the first stage of a two-stage ignition may be considerably reduced or completely eliminated by enhanced initiation of reaction chains. However, the subsequent chemistry and heat release rate of the primary hydrocarbon fuel leading to ignition then becomes controlled by the development of reaction through the alkyl / alkylperoxy radical equilibrium (25). This means that the reaction of aliphatic fuels is automatically, and inevitably, suppressed throughout the temperature range from approximately 750 - 950 K by the predominantly HO_2 propagation regime - which is primarily responsible for the negative temperature dependence of ignition delay exhibited by alkanes and other organic compounds (Fig. 3). The addition of reactive molecular intermediates, such as aldehydes, also suffers from this particular shortcoming. Strategies to overcome this stumbling block have to be established, and these are discussed in Section 6.

There are two features of the role of additives that merit further comment. The first is that nitric oxide, as a secondary product of alkyl nitrate combustion, may have an enhancing role because it is able to sustain the OH radical pool through the reaction

$$HO_2 + NO \rightarrow NO_2 + OH \qquad k_{89} = 2.2 \times 10^{12}\, e^{240/T}\ mol^{-1}\ cm^3\ s^{-1} \quad (89)$$

The second is that the rapid heat release associated with the decomposition and oxidation of peroxides and nitrates, and the fuel oxidation which is promoted by the radical generation, is sufficient to cause quite substantial temperature increase within the reactants [Inomata *et al* (1990)]. The exothermicity is comparable with that from the first stage of a two-stage ignition (which, commonly, is only about 10% of the total enthalpy release on complete combustion to CO_2 and H_2O). This contribution to the enhancement of ignition should not be disregarded, and it might even provide a "stepping stone" to surmount the limitation imposed in the negative temperature dependent regime.

5 NUMERICAL MODELLING AND PROGRESS TOWARDS THE UNDERSTANDING OF THE ROLE OF ADDITIVES

Numerical simulation of the thermokinetic development during combustion provides a powerful route to testing the mechanisms for the effectiveness of additives. Since the temporal development to ignition is of primary concern it is not necessary to explore the behaviour in the context of a fully-developed CFD model to represent a scramjet, or any other practical combustion device. The emphasis on chemical kinetics and heat release, in the form of a detailed model, requires a zero-

dimensional approach. This signifies that there is no spatial variation in concentration or temperature.

The construction of a comprehensive kinetic model to represent the oxidation of a hydrocarbon, incorporating the "best" available kinetic parameters, permits a quantitative link to be forged by numerical computation between detailed chemical measurements and the interpretation of the underlying kinetics and mechanism of the combustion system. For the purpose of validation, the closest experimental approaches are well-stirred, closed or flow systems. The first step is the simulation of composition - time profiles for intermediate and final products under conditions resembling the experimental study, as a validation of the model itself. The prediction of the p-T-composition conditions for ignition, duration of ignition delays and other phenomenology may provide additional support when compared with experimental results. The simulations of the (p-T_a) ignition diagram acetaldehyde combustion using detailed thermokinetic models exemplify the "phenomenological route" [Harrison and Cairnie (1988), Griffiths and Sykes (1989), Kavanagh, Cox and Olson (1990)]. It is necessary also to take heat loss rates into account if ignition occurs in a non-adiabatic system.

Even without comprehensive validation, numerical modelling can prove to be a valuable educational exercise. For example, insight can be gained into the behaviour of free radicals during the course of the reaction, from their predicted profiles. There is also a place for reduced kinetic models in for the prediction of behaviour, as discussed below [Griffiths (1995)].

Even with the zero-dimensional approach, large-scale models with many variables may require considerable computer resource for their implementation, especially under non-isothermal conditions, for which stiffness of the system of differential equations for mass and energy to be integrated is a problem. Comprehensive kinetic models exist for the combustion of alkanes, certainly up to i-octane with some exploration towards the components of kerosene and diesel fuels [Dagaut *et al* (1994)]. The temperature range for the intended application of existing models is approximately 600 - 2600 K. The largest kinetic schemes now run to many thousands of elementary steps. There has been some progress towards an understanding of the reaction mechanisms of benzene and toluene at temperatures above 1000 K, supported by experimental studies [Emdee *et al* (1992)]. A summary of numerical studies up to 1995 is given by Griffiths and Mohamed [1997] and more recent contributions are given in an Appendix.

Of potential relevance as a basis for testing the performance of additives on aviation and related fuels is the model derived by Dagaut *et al* [1995b]. These relate to experimental studies of kerosene oxidation at up to 4 MPa in an isothermal, high pressure CSTR, over the temperature range 750 - 1150 K. A model for n-decane oxidation comprised 90 species in 573 reversible elementary reactions. The principal aim was to reproduce the stationary state concentrations of CO_2, CO, CH_2O, CH_4 and C_2H_4 that were measured experimentally as a function of the reactor temperature at various equivalence ratios, reactant pressures, and mean residence times. This emphasis on low molecular mass species arose because there was substantial experimental evidence that the high molecular mass alkyl radicals,

derived from the predominantly alkane-containing aviation fuel, decomposed readily at temperatures above 750 K to smaller species, as discussed in Section 3a.

It appears that no attention has yet been paid to modelling as a tool for investigating the role of additives using comprehensive kinetic models. However, some indications of the potential for enhancement of ignition by increasing the radical pool for initiation emerge from numerical studies of the combustion of hydrocarbons following rapid compression [Cox *et al* (1996), Curran *et al* (1996)]. The conditions themselves are of peripheral interest to applications in scramjets, but the results are illuminating.

In these papers simulations were made of the ignition delay during spontaneous ignition when n-heptane + air mixtures were compressed rapidly to pressures of about 10 bar and to temperatures (T_c) in the range 650 - 1000 K [Curran *et al* (1996)]. When the temperature and pressure change throughout the compression stroke were included in the calculation, the predicted ignition delays were found to be in very good agreement with the experimental measurements (Fig. 17). Although the compression stroke is sufficiently rapid for virtually adiabatic conditions to be maintained, the time is long enough for reaction to occur during it, such that at the end of the compression small quantities of molecular intermediates are already present in the fuel + air mixture and a pool of free radicals has been created. The effect of this "conditioning" on the ignition delay was demonstrated numerically by then performing the calculation with the end-of-compression temperature and pressure taken to be the initial condition. At $T_c < 800$ K there was no significant difference between the ignition delays predicted by the two methods (Fig. 17). However, increasing extents of the departure between the two were found at higher compressed gas temperatures, to the extent that the predicted ignition delay was about three times longer at $T_c = 930$ K when no conditioning was taken into account.

There has been some exploration using reduced models as a basis for testing additives [Heck (1998)]. Simone Heck [1998] has developed the reduced model by Griffiths *et al* [1994] to apply to alkane isomers in the range C_{10} - C_{16} [Pritchard *et al* (1998)]. The reduced model had been designed in such a way that, with minor adaptation, the behaviour of any alkane isomer could be investigated [Griffiths *et al* (1994)].

Heck [1998] explored the effect of additives on the initiation of ignition of diesel and, for reasons connected with the origins of the model [Griffiths *et al* (1994)], the simulations represented the operating conditions for the rapid compression machine at Leeds (although no experiments has been performed on compounds of these kinds). A mechanism to represent n-octane was set up, since it was found to be less reactive than n-decane and the higher alkanes. Supplementary reactions were then included to represent the decomposition of t-butyl hydroperoxide (t-C_4H_9OOH), *w w'*-azo-toluene ($PhCH_2NNCH_2Ph$), NO_2 and CH_2O. Results from these calculations are given in Table 17.

The decomposition of *w w'*-azo-toluene and the oxidation of the phenyl radicals was modelled by the reactions

$PhCH_2NNCH_2Ph \rightarrow 2PhCH_2 + N_2 \quad k_{90} = 1.22 \times 10^{14} e^{-17500/T}\ s^{-1}$ (90)

$PhCH_2 + O_2 \rightleftharpoons PhCH_2O_2 \quad K_{91} = 1.05 \times 10^{-2} e^{-10360/T}\ mol^{-1}\ cm^3$ (91)

$PhCH_2O_2 \rightarrow PhCHO + OH \quad k_{92} = 1.0 \times 10^{13} e^{-14500/T}\ s^{-1}$ (92)

The rate of reaction (90) is unlikely to be rate determining in this mechanism since the half life of the *w w'*-azo-toluene is 77 μs at 750 K. Thus the rate of generation of OH radicals may be a complex function of the benzyl / benzylperoxy radical equilibrium.

The notional time for the compression stroke was 22 ms. The fuel or fuel + additive mixture was injected to the hot, compressed air at 20 ms, at which the temperature of the air was 745 K. The compression continued for a further 2 ms, and the final temperature under non-reactive conditions was 975 K. An instant evaporation and complete mixing was assumed to have occurred to give a stoichiometric mixture of fuel in air. The compressed gas pressure at the end of the compression stroke was stated to be in the range 20 - 30 atm. Although not clarified, this probably refers to non-reactive conditions. In several cases there was sufficient enhancement to promote ignition at or prior to the end of the compression stroke.

Table 17. Response of n-octane ignition to the addition of additives under a simulated rapid compression [Heck (1998)]

Fuel + additive (% by vol)	t_{ign} / ms (from injection)
$n\text{-}C_8H_{18}$	2.25
$n\text{-}C_8H_{18}$ + 0.01% $t\text{-}C_4H_9OOH$	2.1
$n\text{-}C_8H_{18}$ + 0.1% $t\text{-}C_4H_9OOH$	2.0
$n\text{-}C_8H_{18}$ + 0.01% $PhCH_2NNCH_2Ph$	2.0
$n\text{-}C_8H_{18}$ + 0.1% $PhCH_2NNCH_2Ph$	1.85
$n\text{-}C_8H_{18}$ + 0.001% NO_2	2.23
$n\text{-}C_8H_{18}$ + 0.01% NO_2	2.21
$n\text{-}C_8H_{18}$ + 0.001% CH_2O	2.25
$n\text{-}C_8H_{18}$ + 0.01% CH_2O	2.26
$n\text{-}C_8H_{18}$ + 0.001% (CH_2O + NO_2)	2.24
$n\text{-}C_8H_{18}$ + 0.001% (CH_2O + NO_2)	2.22

No detailed analysis of exactly how the additives were acting was made in this work. However, such small quantities were included that it must be inferred that there is no significant thermal contribution made by the additive decomposition or oxidation. There was found to be a slight retardation by CH_2O. This is likely to have arisen from the replacement of OH by HO_2 through the reactions

$CH_2O + OH \rightarrow HCO + H_2O$ (93)

$HCO + O_2 \rightarrow CO + HO_2$ (94)

The following reactions are thought to give a synergy between CH_2O and NO_2 that partially restores the enhancement of initiation that is achieved by NO_2.

$CH_2O + NO_2 \rightarrow HCO + HNO_2$ (95)

$HNO_2 + M \rightarrow OH + NO + M$ (96)

The preliminary nature of this work indicates that rather more needs to be done for any fundamental conclusions to be drawn from it.

6 STRATEGIES TO PROMOTE ENHANCEMENT OF IGNITION

The formal theoretical background to a unified theory of chain-thermal interactions was set up by Yang and Gray [1965], following a procedure adopted by Sal'nikov [1949], and further developed by them for application to the low temperature combustion of organic compounds [Yang and Gray (1969)]. The principles relate to a two-dimensional representation of criteria for ignition based on the reactant temperature and the concentration of a reactive intermediate in the T-x phase plane. The phase plane is divided by separatrices into regions of ignition and non-ignition, and trajectories on it show the progress from some initial temperature and species concentration to the final steady state of the system (Fig. 18). The phase-plane itself is a time independent representation. The ignition delay is related to the rate of progress along any trajectory onto a common line which approaches a separatrix asymptotically. In its early stages, the rate of progress is tied to the initial conditions for T and x, and it is this part of the process that is susceptible to modification by sensitization. In practice, the behaviour of most systems should be represented by a phase-space, which has n + 1 variables to represent n reactive intermediates and the reactant temperature [Griffiths and Scott (1987)].

The relevance of a radical pool at the initial condition, either to cause ignition or to enhance it, has been addressed analytically and numerically by Creighton and Oppenheim [1986], with specific reference to the $H_2 + O_2$ and $H_2 + F_2$ reactions as examples. They computed integral curves in the T - x phase-plane, where x signifies the total concentration in the free radical pool. The merit of studying hydrogen combustion is that the concentrations of OH and O can, to reasonable approximation, be linked to the H atom concentration through quasi-steady state or partial equilibrium considerations.

There was an earlier experimental and numerical application of the principles of the phase-plane by Levy *et al* [1969] and Cerkanowicz *et al* [1970, 1973], in connection with a US Air Force contracts AFOSR No. F44620-67-C-0068 and F44620-70-C-0051. The combustion of methane and of hydrogen in oxygen were used as examples in this work. The sensitization was caused by the photochemical dissociation of molecular oxygen to O atoms.

More recently, attention has been directed to laser initiation of combustion reactions, both as a thermal input as well a radical source. An example of the former is the computational and experimental study of the ignition of premixed ethene + oxygen mixtures by Tanoff *et al* [1995]. This work also includes an outstandingly good review of preceding theoretical and experimental studies of induced ignition (although the seminal work by Cerkanowicz *et al* was not noted).

As can be surmised from the discussion of the role of additives on hydrocarbon oxidation (Section 4e), a major focus to the enhancement of ignition in hydrocarbon fuels must be to promote more vigorous chain reaction (or chain

branching reaction) over the temperature range approximately 800 - 950 K. The obstacle in the unperturbed oxidation processes is the domination of HO_2 chain propagation for both aliphatic and aromatic hydrocarbons. Even the vigorous reaction of alkanes at lower temperatures is overtaken by this sluggish chemistry, with its inherently low radical pool. The difficulty associated with the commonly used promoters for diesel fuels (e.g. organic peroxides and nitrates) is that they have their greatest effect at temperatures lower than this crucial regime because they decompose so readily. A compensation may be the supplementary thermal contribution that accompanies the reaction of the additive [Inomata *et al* (1990)].

The laser induced decomposition of H_2O_2 during the two-stage ignition of n-heptane, stabilised on a flat flame burner [Morley (1988)], shows how, at temperatures above 800 K between the first and second stage, excess OH radicals are forced to decay to their quasi-steady equilibrium concentration (i.e. to the unperturbed trajectory in the T - x phase space) rather than enhance the second stage processes.

The requirements to bring about an escalation of the reaction rate in the unreactive regime (800 - 900 K) is either through the continuous generation of additional free radicals or the recycling of reactive intermediates, each of which must occur independently of the main propagating chain. There is an attraction of H atom generation in this role because of the potential for chain branching *via*

$$H + O_2 \rightarrow OH + O \qquad (64)$$

but the competition with the association reaction

$$H + O_2 + M \rightarrow HO_2 + M \qquad (66)$$

must always be taken into account, especially at operating pressures where reaction (66) will be dominant (see Fig. 16 and Section 3h).

A potentially more successful species to be introduced to the radical pool would be the O atom, because it is capable of generating new reaction chains *via*

$$O + RH \rightarrow OH + R \qquad (65)$$

Ozone is a candidate for O atom generation, which might be practical in terrestrial applications. The complications of its use arise from the need for *in situ* generation by electric discharge in a flow system, followed by injection at an appropriate stage of reaction. The promotion of the gas-phase oxidation of alkanes by ozone at low temperatures has been studied in a CSTR (Caprio *et al* (1979)]. In the absence of species with which O atoms may react, ozone decomposes exceedingly readily according to the mechanism [Benson and Axworthy (1957)]

$$O_3 + M \rightleftharpoons O_2 + O + M \qquad k_{97f} = 4.6 \times 10^{12}\, e^{-12000/T}\ mol^{-1}\ dm^3\ s^{-1} \qquad (97)$$
$$k_{97b} = 6.0 \times 10^{7}\, e^{300/T}\ mol^{-2}\ dm^6\ s^{-1}$$

$$O + O_3 \rightarrow 2O_2 \qquad k_{98} = 3.0 \times 10^{10}\, e^{-3000/T}\ mol^{-1}\ dm^3\ s^{-1} \qquad (98)$$

Other photolytic methods have been used in for the formation of O atoms in chemical kinetic studies, such as by the mercury sensitised photolysis of O_2 [Volman (1963)] or the photolysis of CO_2 at a wavelength of 147 nm [Jucker and Rideal (1957)].

With the exception of reaction (64), other chemical routes to the generation of O atoms have yet to be designed, although there are other possibilities in the context of hydrocarbon oxidation chemistry. For example the reaction [Tanoff *et al* (1995)]

$$CH + O_2 \rightarrow HCO + O \qquad k = 1.0 \times 10^{13}\ mol^{-1}\ cm^3\ s^{-1} \quad (99)$$

is believed to compete successfully with

$$CH + O_2 \rightarrow CO + OH \qquad k = 1.35 \times 10^{11} T^{0.67}\ e^{-12850/T}\ mol^{-1}\ cm^3\ s^{-1} \quad (100)$$

Thus if the formation of CH could be induced by chemical means an enhancement of O atom concentrations might follow from this. CH_2 would be the pre-cursor to this, for which ketene (CH_2CO) might be a source, albeit involving a photolytic decomposition [Calvert and Pitts (1966)]. The combustion of ketene in oxygen has been investigated over the temperature range 600 - 800 K [Michaud *et al* (1965)].

There may also be possibilities of exploiting the reaction

$$N + O_2 \rightarrow NO + O \quad (101)$$

if it is preceded by the "prompt NO" process

$$CH + N_2 \rightarrow HCN + N \quad (102)$$

Reactions that are believed to be involved in the oxidation of fuel-bound nitrogen may also be utilised in the generation of O atoms from selected additives, such as [Etzkorn *et al* (1994)]

$$NH + O_2 \rightarrow HNO + O \qquad k = 3.8 \times 10^{10}\ e^{-770/T}\ mol^{-1}\ cm^3\ s^{-1} \quad (103)$$

$$CN + O_2 \rightarrow NCO + O \qquad k = 6.6 \times 10^{12}\ e^{204/T}\ mol^{-1}\ cm^3\ s^{-1} \quad (104)$$

Reactions of these kinds may be contributory to diethylamine as a successful promoter of ignition of alkanes at temperatures above 850 K [Mohamed (1998)]. At 900 K a reduction of 50% was measured in the ignition delay of n-pentane when 5% by volume diethylamine was present. However, amines are known to retard the oxidation of alkanes at lower temperatures [Cullis and Waddington (1957)], possibly through the abstraction of the labile H atom from the N-H group to leave a relatively stable free radical.

Boron assisted combustion, as an augmentation of O atoms and chain branching, has also been explored, but it seems not to be effective at temperatures below 1800 K [Yetter *et al* (1988)].

Finally, there has been considerable development in the understanding of initiation by a surface catalysed reactions, which may offer a novel route to the accumulation of a radical pool in the gas phase [Song *et al* (1990)].

7 REFERENCES

Agnew, J.T., Agnew, W. J. and Wark, K., *Sixth Symposium (International) on Combustion*, The Combustion Institute (1957), p 894

Agnew, W.G. and Agnew, J.T., *Tenth Symposium (International) on Combustion*, The Combustion Institute (1965), p 123

Al-Rubaie, M.AR., Griffiths, J.F. and Sheppard, C.G.W., *SAE Technical paper* 912333 (1991)

Baldwin, R.R. and Walker, R.W., *Eighteenth Symposium (International) on Combustion*, The Combustion Institute (1981), p 819

Baldwin, R.R., Scott, M. and Walker, R.W., *Twenty-First Symposium (International) on Combustion*, The Combustion Institute (1986), p 991

Ballinger, P.R. and Ryason, P.R., *Thirteenth Symposium (International) on Combustion*, The Combustion Institute (1971), p 271

Baulch, D.L., Cobos, C.J., Cox, R.A., Esser, C., Frank, P., Just, Th., Kerr, J.A., Pilling, M.J., Troe, J., Walker, R.W. and Warnatz, J., *J. Phys. Ref. Data*, **21**, 411 (1992)

Beatty, H.A. and Edgar, J., *J. Am. Chem. Soc.*, **56**, 102 (1934)

Beeley, P.B., Griffiths, J.F. and Gray, P., *Combust Flame*, **39**, 255 (1980a)

Beeley, P.B., Griffiths, J.F. and Gray, P., *Combust Flame*, **39**, 269 (1980b)

Benson, S.W. and Axworthy, A.E. *J. Chem Phys.*, **26**, 1718 (1957)

Burcat, A., Lifshitz, A., Scheller, K. and Skinner, G.B., *Thirteenth Symposium (International) on Combustion*, The Combustion Institute (1970). p 745

Braun-Unkhoff, M., Frank, P. and Just, Th., *Twenty-Second Symposium (International) on Combustion*, The Combustion Institute (1989), p 1053

Brezinsky, K., Burke, E.J. and Glassman, I., *Twentieth Symposium (International) on Combustion*, The Combustion Institue (1984), p 613

Brezinsky, K., Linteris, G.T., Litzinger, T.A. and Glassman, I., *Twenty-First Symposium (International) on Combustion*, The Combustion Institute (1986), p 833

Brezinsky, K., *Prog. Energy Combust. Sci.*, **12**, 1 (1986)

Cadman, P., Ninteenth International Shock Wave Symposium (1993)

Calvert, J.G. and Pitts Jr., J.N., *Photochemistry*, John Wiley, New York (1966)

Cavanah, J., Cox, R.A. and Olson, G., *Combust. Flame*, **82**, 15 (1990)

Cavaliere, A., Ciajolo, A., D'Anna, A., Mercogliano, R. and Ragucci, R., *Combust. Flame*, **93**, 279 (1993)

Ciezki, H.K. and Adomeit, G, *Combust. Flame*, **93**, 421 (1993)

Caprio, V., Insola, A. and Lignola, P.G., *Comb. Sci. Tech.*, **20**, 19 (1979)

Caprio, V., Insola, A. and Lignola, P.G., *Combust. Flame*, **43**, 23 (1981)

Carlier, M., Corre, C., Minetti, R., Pauwels, J-F., Ribaucour, M. and Sochet, L-R., *Twenty-Third Symposium (International) on Combustion* , The Combustion Institute (1990), p 1753

Cerkanowicz, A.E., Levy, M.E. and McAlevy III, R.F., *AIAA paper*, **70-149** (1970)

Cerkanowicz, A.E., Levy, M.E. and McAlevy III, R.F., *AIAA paper*, **73-216** (1973)

Clothier, P.Q.E., Aguda, B.D., Moise, A. and Pritchard, H.O., *Chem. Soc. Rev.* (1993)

Cox, A., Griffiths, J.F., Mohamed, C., Curran, H.J., Pitz, W.J. and Westbrook, C.K., *Twenty-Sixth Symposium (International) on Combustion* , The Combustion Institute (1996), p 2685

Creighton, J.R. and Oppenheim, A.K., *Proceedings of 10th ICDERS*, AIAA, 304 (1986)

Cullis, C.F. and Waddington, D.J., *Trans. Faraday Soc.*, **53**, 1371 (1957)
Curran, H.J., Griffiths, J.F., Mohamed, C., Pitz, W.J. and Westbrook, C.K., *Third Symposium on Numerical Modelling,* Heidelberg, 1996.
Dagaut, P., Reuillon, M. and Cathonnet, M., *Comb. Sci. Tech.*, **95**, 233 (1994a)
Dagaut, P., Reuillon, M. and Cathonnet, M., *Comb. Sci. Tech.*, **103**, 349 (1994b)
Dagaut, P., Reuillon, M. and Cathonnet, M., *Combust. Flame.*, **132**, 101 (1995a)
Dagaut, P., Reuillon, M., Boettner, J.C. and Cathonnet, M., *Twenty-Fifth Symposium (International) on Combustion* , The Combustion Institute (1995b), p 919
Dryer, F.L. and Glassman, I., *Fourteenth Symposium (International) on Combustion*, The Combustion Institute (1973), p 987
Dryer, F.L. and Brezinsky, K., *Combust. Sci. Tech.,* **45**, 199 (1986a)
Dryer, F.L. and Brezinsky, K., *Combust. Sci. Tech.*, **45**, 225 (1986b)
Emdee, J.L., Brezinsky, K. and Glassman, I., *Twenty-Third Symposium (International) on Combustion*, The Combustion Institute (1990), p 77
Emdee, J.L., Brezinsky, K. and Glassman, I. *J. Phys. Chem.*, 96, 2151 (1992)
Etzkorn, T., Muris, S., Wolfrum, J., Bockhorn, H., Nelson, P.F., Attia-Shahin, A. and Warnatz, J., *Twenty-Fourth Symposium (International) on Combustion*, The Combustion Institute (1992), p 925
Fenter, F.F., Nozier, B., Caralp, F. and Lesclaux, K., *Int. J. Chem. Kin.*, **26**, 171 (1994)
Fish, A., Haskell, W.W. and Read, I.A., *Proc. Roy. Soc. Lond. A*, **313**, 261 (1969)
Gray, P., Griffiths, J.F. and Hasko, S.M., *Proc. R. Soc. Lond. A.*, **396**, 227 (1984
Goodger, E.M. and Eissa, A.F.M., *J. Inst. Energy*, 84 and 199 (1987)
Griffiths, J.F, *Prog. Energy Combust. Sci.*, **21**, 25 (1995)
Griffiths, J.F., Gilligan, M.F. and Gray, P., *Combust. Flame*, **26**, 385 (12976)
Griffiths, J.F., Halford-Maw, P.A. and Rose, D.J., *Combust. Flame*, **95**, 291 (1993)
Griffiths, J.F., Halford-Maw, P.A. and Mohamed, C., *Combust. Flame*, **111**, 327 (1997)
Griffiths, J.F., Hasko, S.M., Shaw, N.K. and Torres-Mujica, T., *J. Chem. Soc., Faraday Trans. I*, **81**, 343 (1985)
Griffiths, J.F., Hughes, K.J.., Schreiber, M. and Poppe, C., *Combust. Flame*, **99**, 533 (1994)
Griffiths, J.F., Jiao, Q., Kordylewski, W., Schreiber, M., Meyer, J. and Knoche, K.F., *Combust. Flame*, **93**, 303 (1993)
Griffiths, J.F. and Mohamed, C., "Chapter 6, Experimental and numerical studies of oxidation chemistry", in *Comprehensive Chemical Kinetics, Vol 35*, R.G. Compton and G. Hancock (eds.), Elsevier, Amsterdam, 1998, p545
Griffiths, J.F. and Mullins, J.R., *Combust. Flame*, **56**, 135 (1984)
Griffiths, J.F. and Phillips, C.H., *Combust. Flame*, **81**, 304 (1990)
Griffiths, J.F. and Scott, S.K., *Prog. Energy Combust. Sci.*, **13**, 161 (1987)
Griffiths, J.F. and Singh, H.J., *J. Chem. Soc., Faraday Trans I*, **78**, 747 (1982)
Griffiths, J.F., Skirrow, G. and Tipper, C.F.H., *Combust. Flame*, **12**, 443 (1968)
Griffiths, J.F. and Sykes, A.F., *Proc. R. Soc. Lond. A*, **422**, 289 (1989)
Gulati, S.K. and Walker, R.W., *J. Chem. Soc. Faraday Trans.* 2, **85**, 1799 (1989)
Handford-Styring, S. and Walker, R.W., *J. Chem. Soc. Faraday Trans.*, **91**, 1431 (1995)
Harrison, A.J. and Cairnie, L.R., *Combust. Flame*, **71**, 1 (1988)
Heck, S., "Spontaneous Ignition of Hydrocarbons", *PhD Thesis*, York University, Ontario (1998)

Inomata, T., Griffiths, J.F. and Pappin, A.J., *Twenty-Third Symposium (International) on Combustion*, The Combustion Institute (1990), p 1759
Jost, W., *Third Symposium on Combustion*, The Combustion Institute (1949), p 424
Jucker, H. and Rideal H.K., *J. Chem. Soc.* 1058 (1957)
Koert, D.N., Miller, D.L. and Cernansky, N.P., *Combust. Flame*, **96**, 34 (1994)
Levy, M.E., Cerkanowicz, A.E. and McAlevy III, R.F., *AIAA paper*, **69-88** (1969)
Lewis, B. and von Elbe, G., *Flames, Combustion and Explosion in Gases, Third Edition*, Academic Press, New York, 1978
Li, T.M. and Simmons, R.F., *Twenty-First Symposium (International) on Combustion* , The Combustion Institute (1986), p 455
Lignola, P.G., Reverchon, E. and Balzano, M., *Combust. Flame*, **51**, 19 (1983)
Lignola, P.G., Di Maio, F.P., Marzocchella, A. and Mercogliano, R., *Twenty-Second Symposium (International) on Combustion*, The Combustion Institute, Pittsburgh, (1988) p 1625
Martinengo, A., *Oxidation.and Combustion Reviews.,Vol 2*, Ed. C.F.H.Tipper, Elsevier, Amsterdam (1967), p 207
Michaud, P., Lebel, J. and Ouellet, C., *Combust. Flame*, **12**, 395 (1965)
Minetti, M., Carlier, M., Ribaucour, M., Therssen, E. and Sochet, L-R., *Combust. Flame*, in press (1995)
Mohamed, C., *Combust. Flame*, **112**, 438 (1998)
Morley, C., *Twenty-Second Symposium (International) on Combustion* , The Combustion Institute (1989), p 911
Pease, R.N., *J. Am. Chem. Soc.*, **51**, 1839 (1929)
Pedler, A.E. and Pollard, F.H., *Trans. Faraday Soc.*, **53**, 44 (1957)
Poppe, C., Schreiber, M., and Griffiths, J.F., *British, French and German Section Meeting of the Combustion Institute*, Cambridge (1993)
Pritchard, H.O. *Combust. Flame*, **75**, 415 (1989)
Pritchard, H.O., Heck, S. and Griffiths, J.F., *J. Chem. Soc. Faraday Trans.*, in press (1998)
Rocha, W.D., *MSc Diss.*, University of Leeds , 1996
Sahetchian, K.A., Rigny, R. and Circan, S., *Combust. Flame*, **85**, 511 (1991)
Salnikov, I.E., *Zh. Fiz. Khim.*, **23**, 258 (1949)
Shaddix, C.R., Brezinsky, K. and Glassman, I., *Twenty-Fourth Symposium (International) on Combustion*, The Combustion Institute (1992), p 683
Snee, T.J. and Griffiths, J.F., *Combust. Flame*, **75**, 381 (1989)
Song, X., Williams, W.R., Schmidt, L.D. and Aris, R., *Twenty-Third Symposium (International) on Combustion*, The Combustion Institute (1990), p 1129
Spadaccini, L.J. and Colket, M.B., *Prog. Energy Combust. Sci.*, **20**, 431 (1994)
Spence, K. and Townend, D.T.A., *Third Symposium on Combustion*, The Combustion Institute, Pittsburgh (1949), p 404
Sokolik, A.S., *Self-Ignition, Flame and Explosion of Gases*, Israel Program for Scientific Translations, Jerusalem (1963)
Stothard, N.D. and Walker R.W., *J. Chem. Soc. Faraday Trans.*, **88**, 2621 (1991)
Tanoff, M.A., Smooke, M.D., Teets, R.E. and Sell, J.A., *Combust. Flame*, **103**, 253 (1995)
Thornton, M.M., Malte, P.C. and Crittenden, A.L., *Twenty-First Symposium (International) on Combustion*, The Combustion Institute (1986), p 979
Venkat, C., Brezinsky, K. and Glassman, I., *Nineteenth Symposium (International) on Combustion*, The Combustion Institute (1982), p 143

Volman, D.R., *Adv. in Photochemistry, Vol. 1*, eds. W.A. Noyes Jr., G.S. Hammond and J.N. Pitts Jr., John Wiley, New York, 1963, p52
Walker, R.W. and Morley, C., "Chapter 1, Basic chemistry of combustion", in *Comprehensive Chemical Kinetics, Vol 35*, R.G. Compton and G. Hancock (eds.), Elsevier, Amsterdam, 1998, p1
Warnatz, J., *Twentieth Symposium (International) on Combustion*, The Combustion Institute (1984), p 845
Westbrook, C.K., Pitz, W.J., Thornton, M.M. and Malte, P.C., *Twenty-Second Symposium (International) on Combustion*, The Combustion Institute (1988), p 863
Williams, F.W., Sheinson, R.S., Bogan, D.J. Rabitz, H.A. and Indritz, D., *Eastern States Section of the Combustion Institute*, 1976
Williams, K.G., Johnson, J.E. and Carhart, H.W., *Seventh Symposium (International) on Combustion*, The Combustion Institute (1959), p 392
Yang, C.H. and Gray, B.F., *J. Phys. Chem.*, **69**, 2747 (1965)
Yang, C.H. and Gray, B.F., *J. Phys. Chem.*, **73**, 3395 (1965)
Yetter, R.A., Cho, S.Y., Rabitz, H., Dryer, F.L., Brown, R.C. and Kolb, C.L., *Twenty-Second Symposium (International) on Combustion*, The Combustion Institute (1988), p 926
Zeelenberg, A.P. and de Bruijn, H.W., *Combust. Flame*, **3**, 281 (1965)

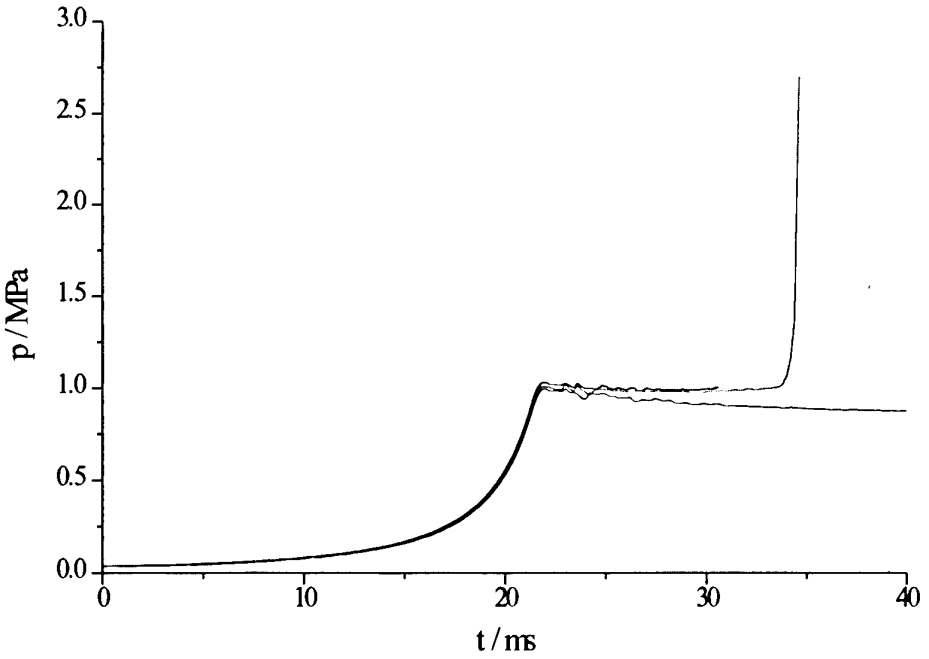

Figure 1. Pressure records during the single-stage ignition of n-pentane + air (ϕ = 1) up to and following compression to 900 K at a gas density of 128 mol m^{-3}. The compression of n-pentane + inert gas is also shown. Heat loss to the chamber walls causes the fall in pressure after the end of compression. The difference between the reactive and non-reactive cases results from heat release during the induction period and at ignition.

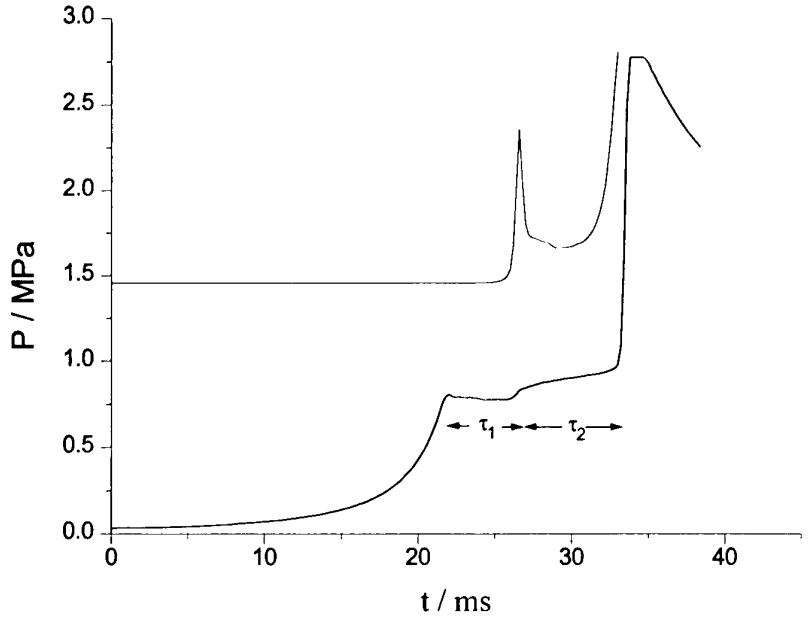

Figure 2. Pressure (lower) and light output (upper) records during the two-stage ignition of n-pentane + air mixtures (ϕ = 1) in a rapid compression machine. The compressed gas temperature and density were 740 K and 128 mol m^{-3} respectively. The initial peak in the light output was caused by emission from CH_2O^* and it is associated with the very weak "cool flame" activity.

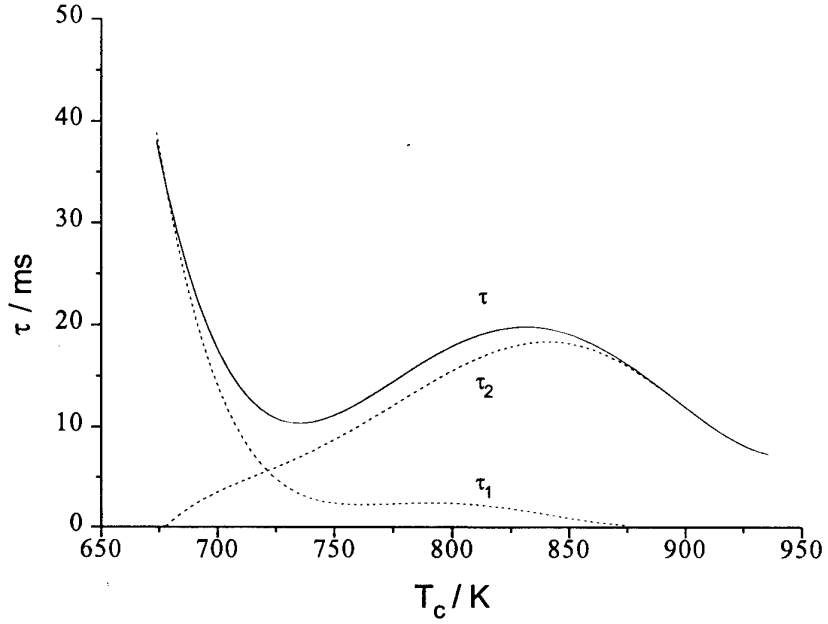

Figure 3. Ignition delay (τ) of n-pentane + air mixtures at ϕ = 1 in a rapid compression machine plotted as a function of compressed gas temperature (T_c). The compressed gas density was 128 mol m^{-3}. The ignition delay is divided into two regions, distinguished as the first stage, τ_1 and the second stage τ_2 (see Fig. 2).

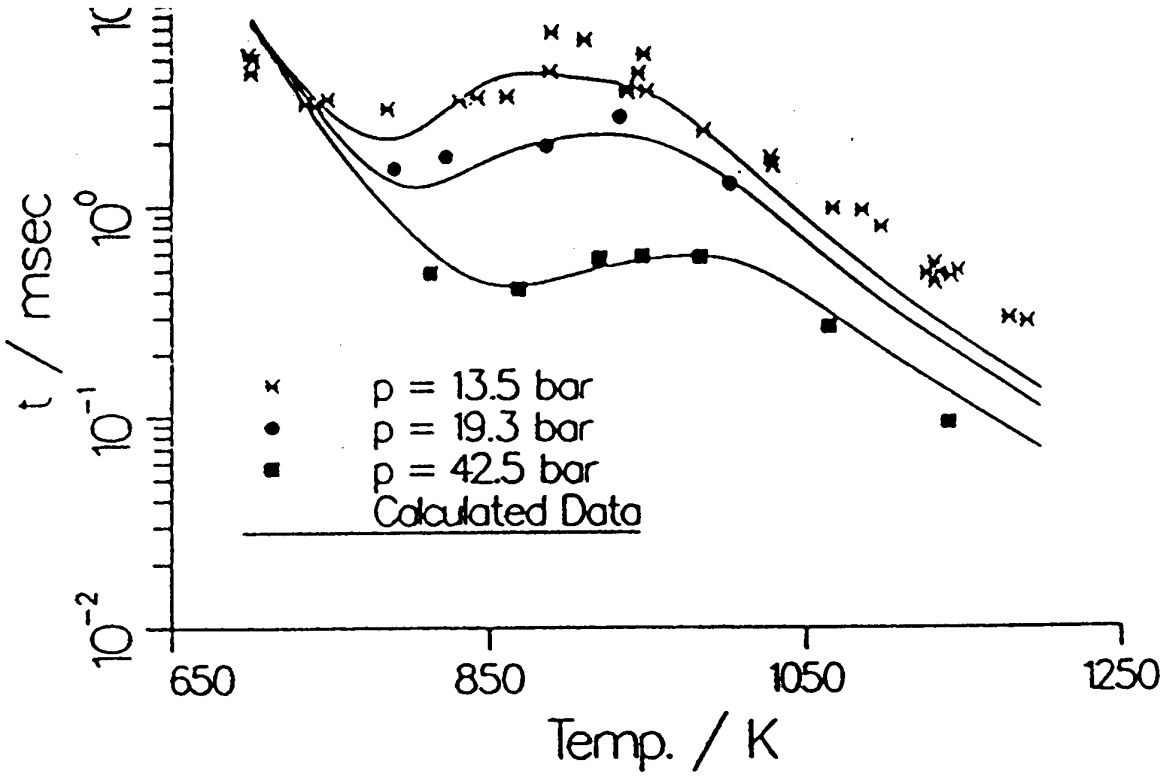

Figure 4 Ignition delays for n-heptane + air mixture (f = 1) obtained in a shock tube at three different shocked gas pressures [Ciezki and Adomeit (1993)]. The negative temperature dependence of the ignition delay at temperatures above 800 K can be clearly seen in these results.

Figure 5 Ignition delays for n-tetradecane obtained in a flow system [Cavaliere *et al* (1993)].

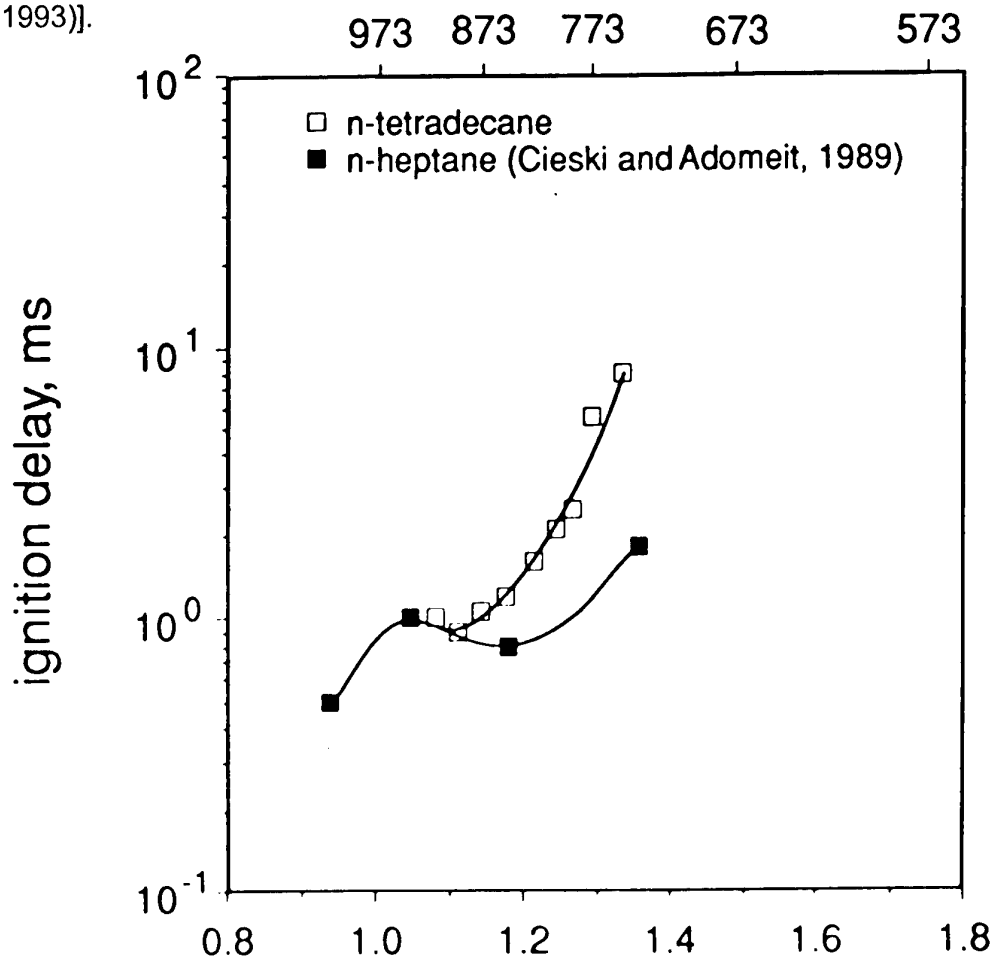

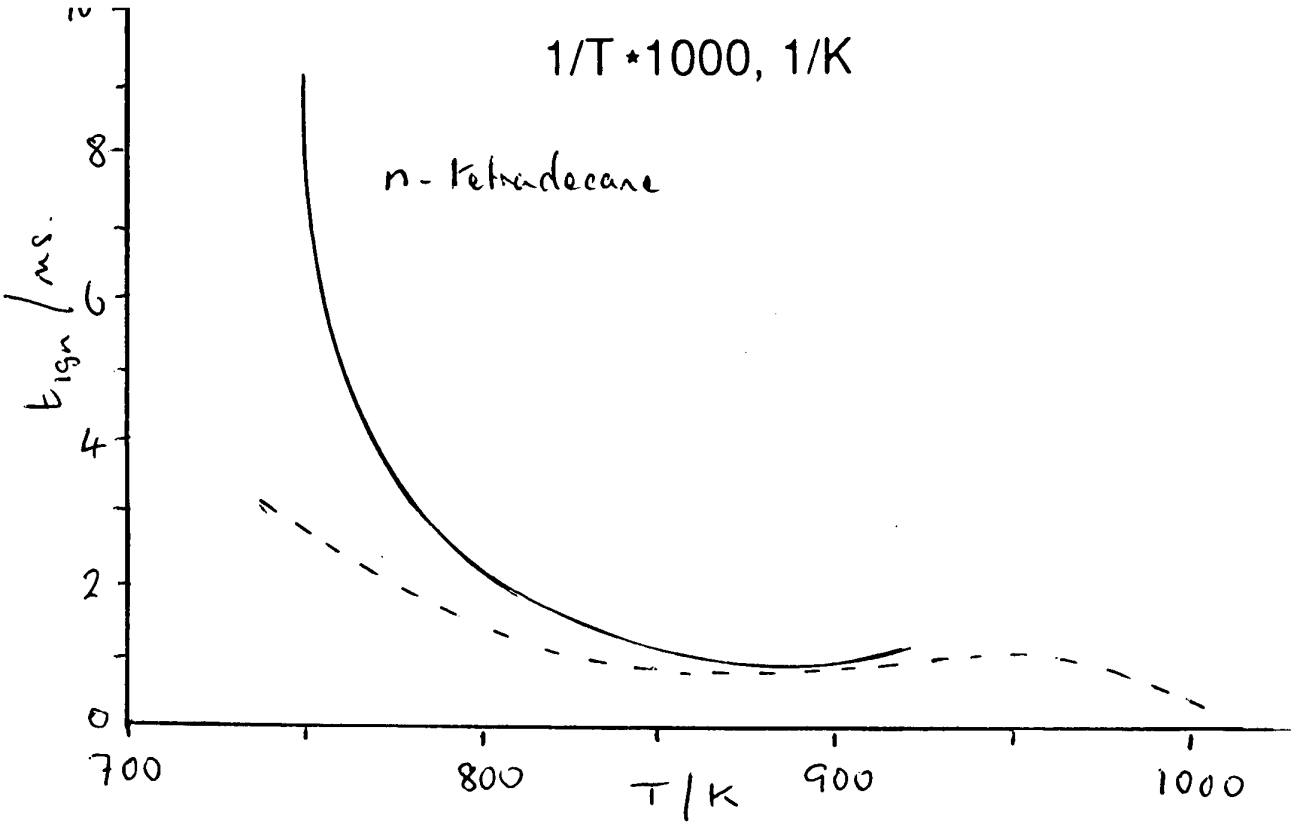

Figure 6 Ignition delays for n-heptane, i-octane, kerosine and gas oil measured for a single drop fallling through a hot enclosure [Goodger and Eissa (1987)]

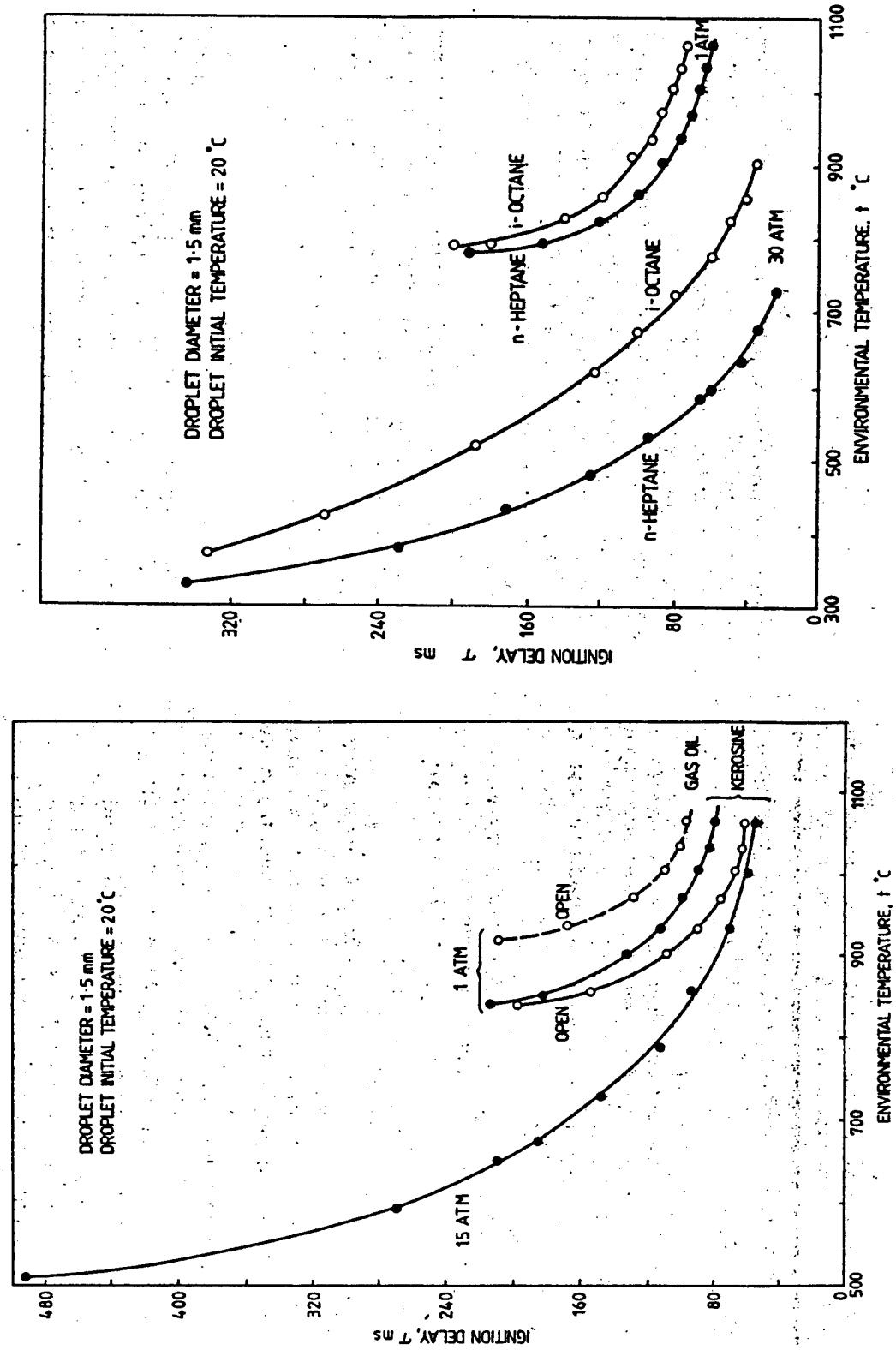

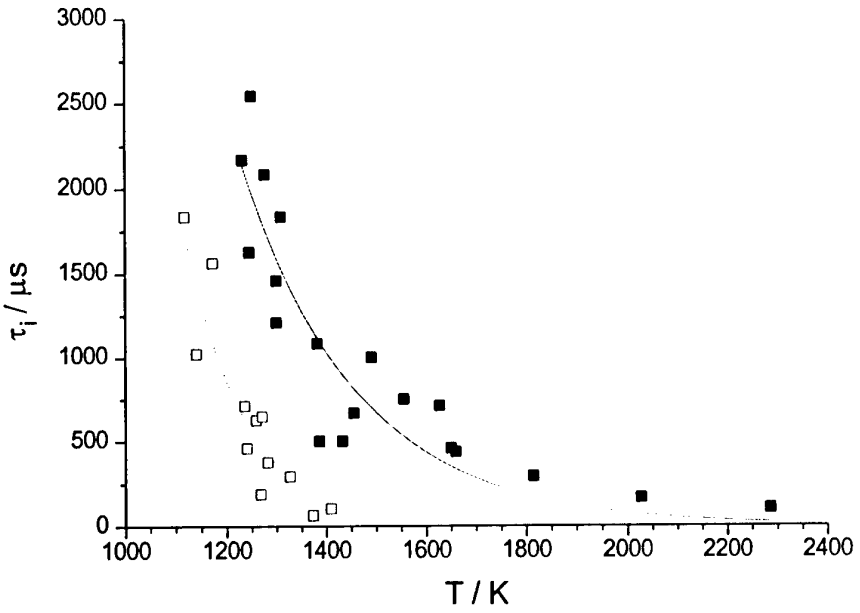

Figure 7 Ignition delays for toluene + air at ϕ = 1 measured behind a reflected shock wave. The shocked gas pressures were 0.5 - 0.7 bar (closed symbols) and 1.7 - 2.0 (open symbols) respectively [Cadman (1993)]

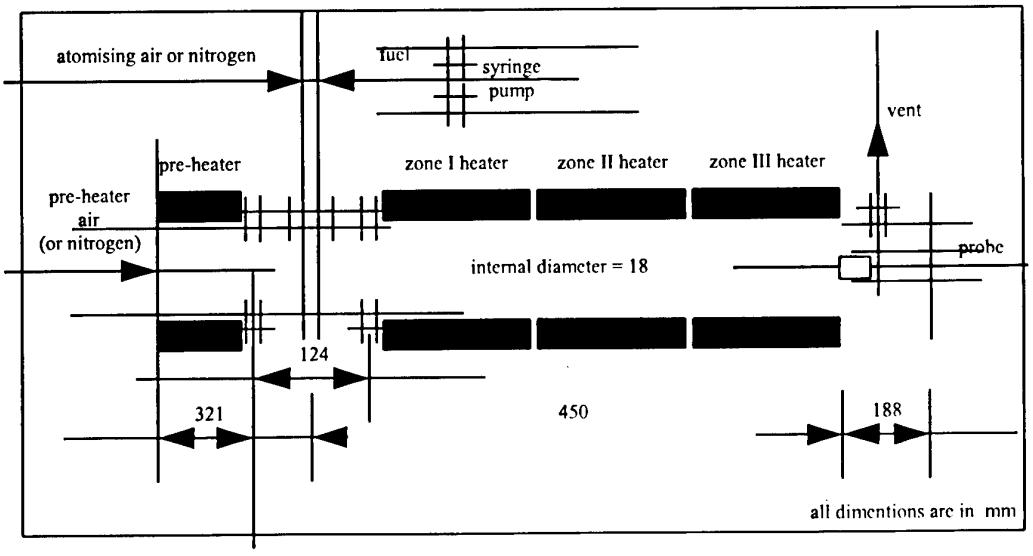

Figure 8 Schematic representation of the Leeds flow system for testing additive performance

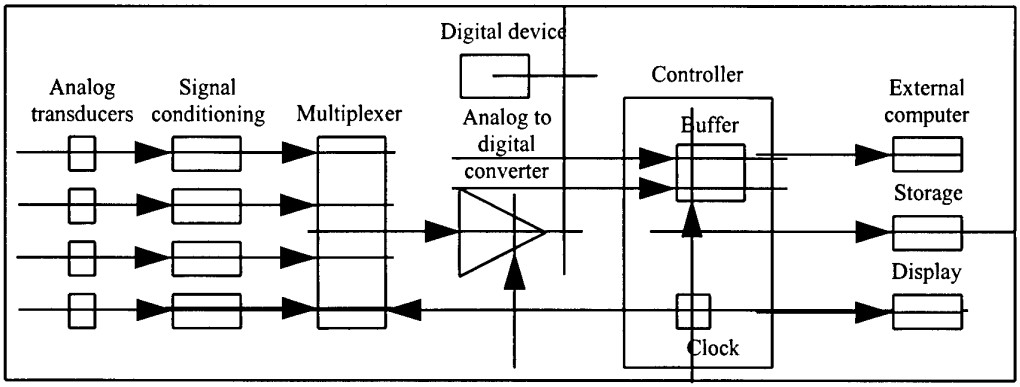

Figure 9. Signal flow scheme for data acquisition system

Run No : F86 DIESEL FLOW RIG (DFR2) Date : 23 Jul

Comment : T 630, 420, 380, 375, dwell time 120

Fuel Type : 1-Octene + 0.5% IPN

Air Temp	25.2	°C
N2 Temp	22.3	°C
Fume Cupboard Max Temp	20.4	°C
Fume Cupboard Min Temp	20.1	°C
Pre Heater Temp	630	°C
Tube Furnace Zone 1	420	°C
Tube Furnace Zone 2	380	°C
Tube Furnace Zone 3	375	°C
Fuel Flow	40.0	ml/hr
Fuel Density @ 20 °C	0.7149	g/ml
Pre Heater Air Flow	160.0	ml/sec
Pre Heater N2 Flow	0.0	ml/sec
Atomiser Air Flow	40.0	ml/sec
Total Gas Vol Flow	200.0	ml/sec
Fuel Carbon	85.71	%
Fuel Hydrogen	14.29	%
Fuel Sulphur	0.00	%
Stoichiometric Ratio	14.69	
Initial O2	21.2	%
Initial CO	.24	%
Initial CO2	.14	%
Air : Fuel Ratio	29.6 :1	
Ignition Delay Time	7.8	ms

Probe Position mm	Baseline °C	Fuel Run °C	Temp Diff °C	Residence Time ms	O2 %	CO %	CO2 %
0	424.1	409.6	-14.5	0.0	20.7	1.03	.16
10	425.3	422.0	-3.3	5.0	20.7	1.03	.15
20	423.0	425.5	2.5	9.9	20.7	1.03	.15
35	414.3	423.9	9.6	17.5	20.7	1.03	.15
50	407.8	420.8	13.0	25.1	20.6	1.03	.15
75	401.6	419.6	18.0	37.9	20.6	1.03	.15
100	405.4	429.6	24.2	50.7	20.5	1.03	.15
125	411.3	440.8	29.5	63.4	20.5	1.03	.16
150	417.3	452.8	35.5	76.0	20.4	1.03	.16
200	422.8	460.0	37.2	101.0	20.4	1.03	.15
250	419.9	457.0	37.1	126.0	20.4	1.03	.14
300	417.1	454.4	37.3	151.1	20.4	1.03	.14
350	414.8	451.3	36.5	176.2	20.4	1.03	.14
400	412.8	446.4	33.6	201.5	20.5	1.03	.14
450	410.0	441.7	31.7	226.8	20.5	1.03	.13

Figure 10. A Typical Test Print-out

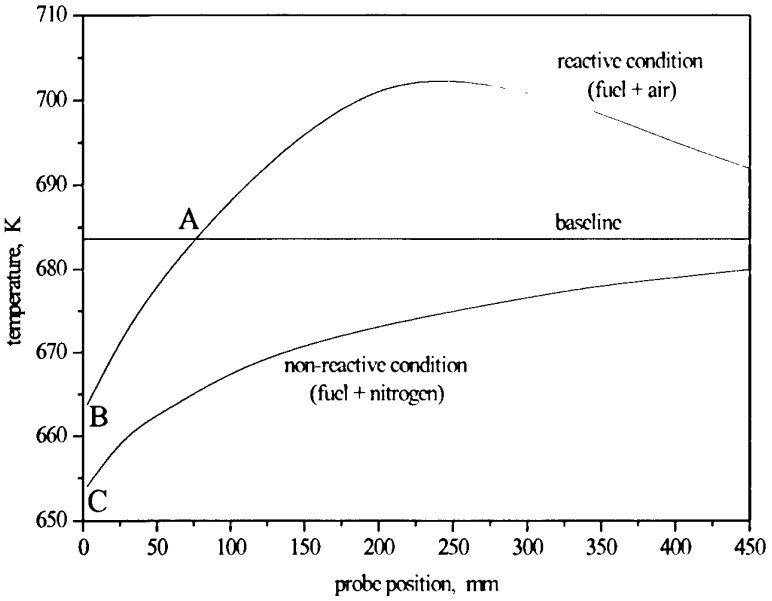

Figure 11 Typical temperature -position profiles from for reactive (B) and non-reactive (C) flow conditions. The baseline represents the no-flow profile.

Figure 12 ΔT distance profiles obtained in the Leeds flow system during the combustion of 1-octene with increasing proportions (by vol) of di-t-butyl peroxide (DTBP) added to it. A comparison with n-heptane is included.

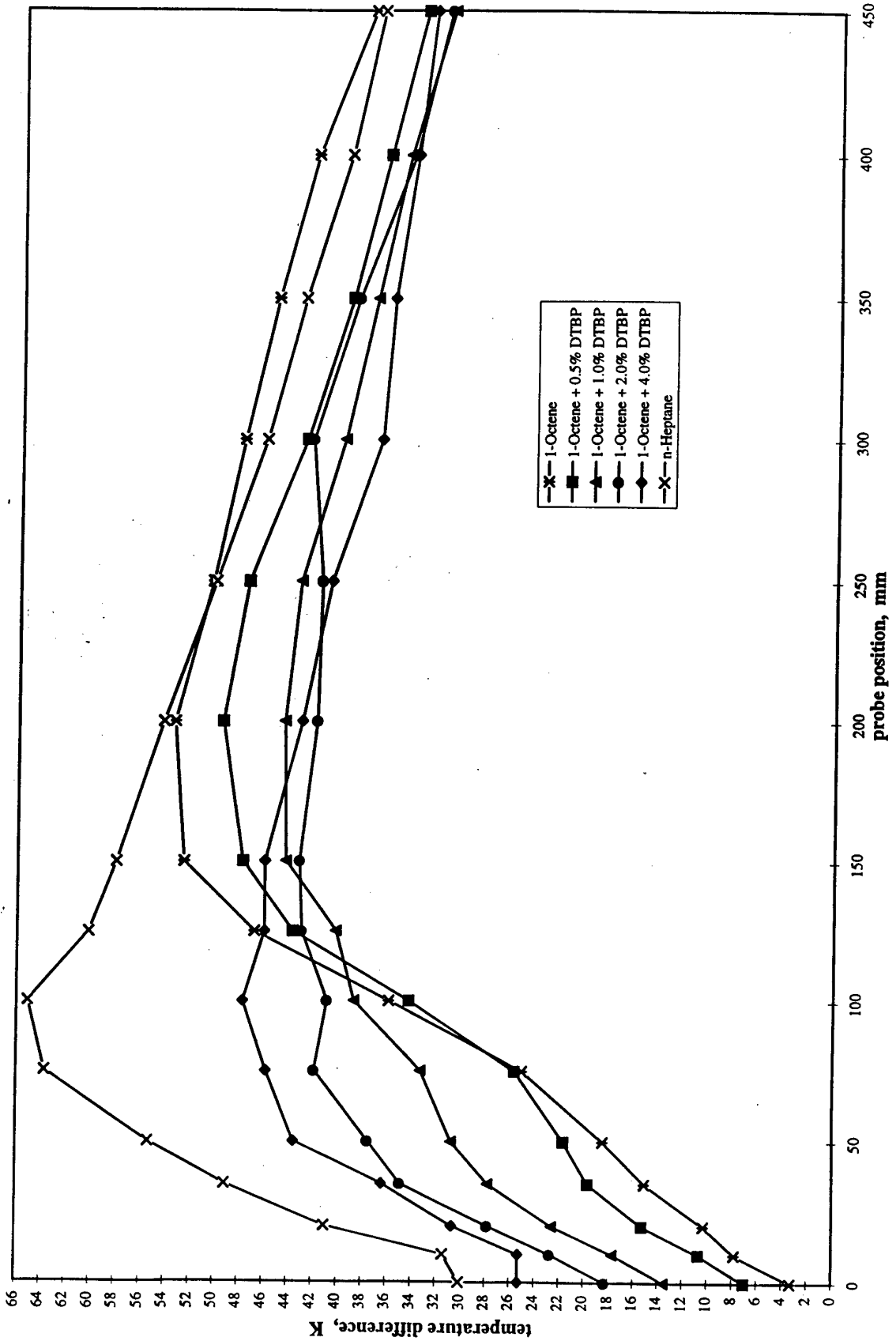

Figure 13 ΔT distance profiles obtained in the Leeds flow system during the combustion of 1-octene with increasing proportions (by vol) of isopropyl nitrate (IPN) added to it. A comparison with n-heptane is included.

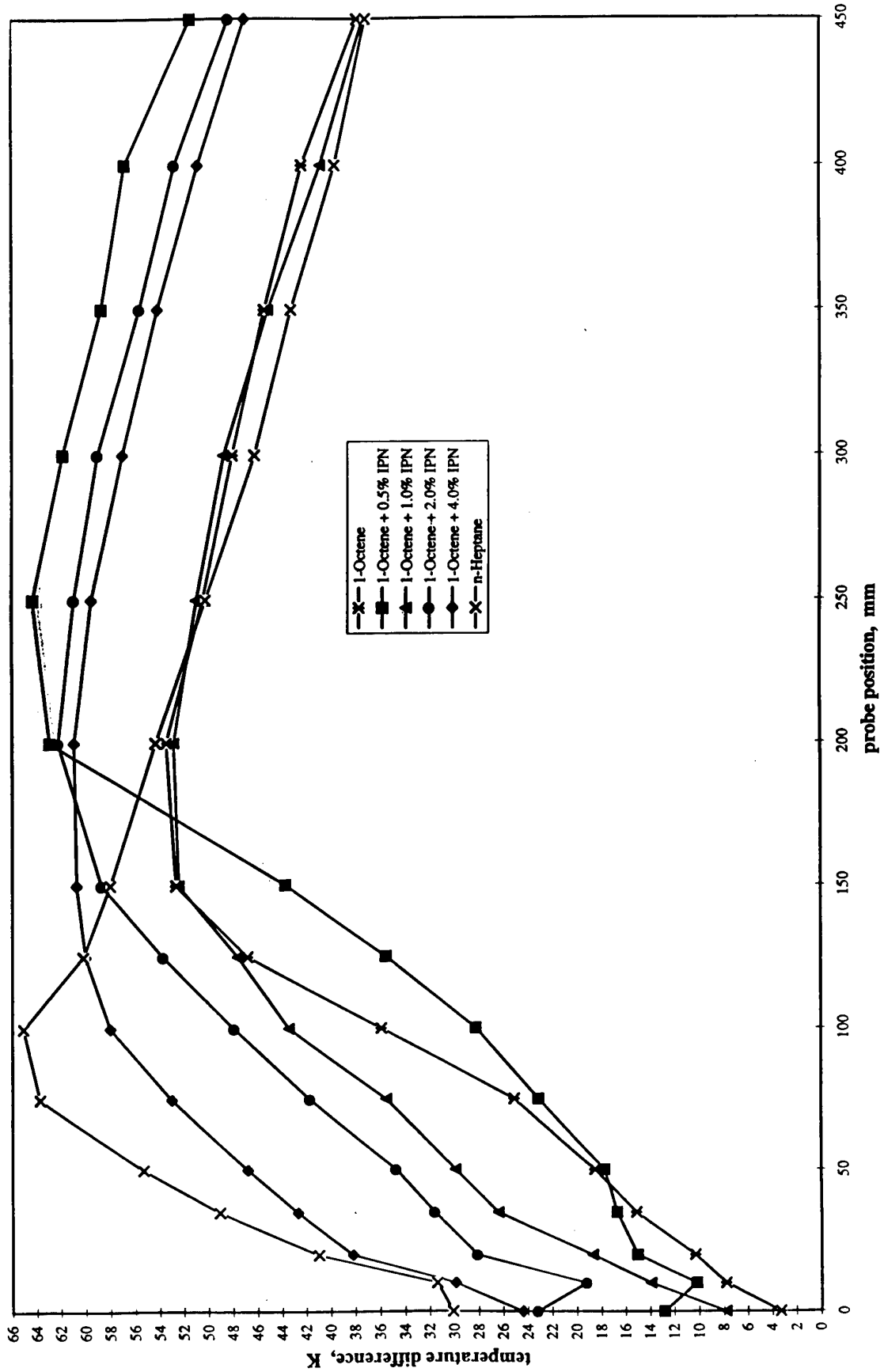

Figure 14 An overview of the mechanisms of oxidation for alkanes at temperatures below 1000 K [Walker and Morley (1996)].

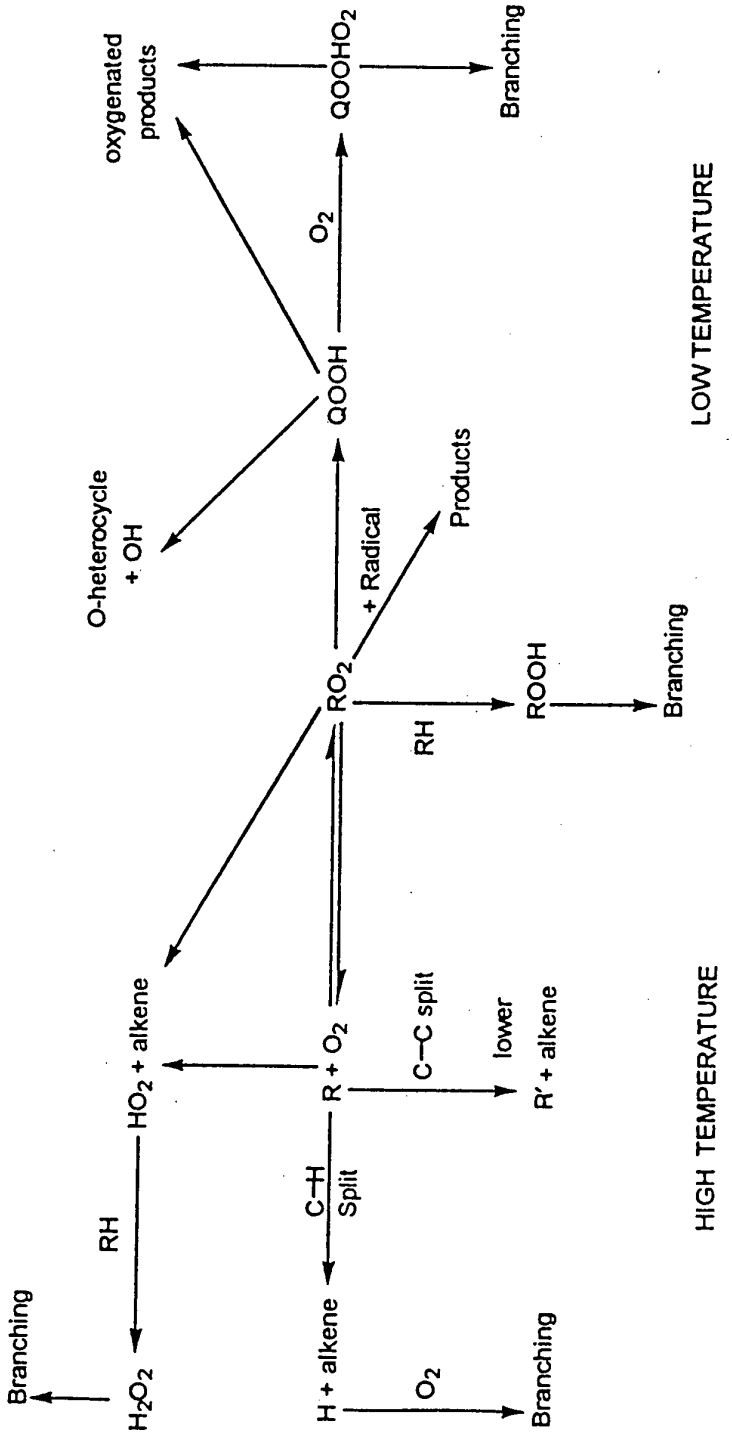

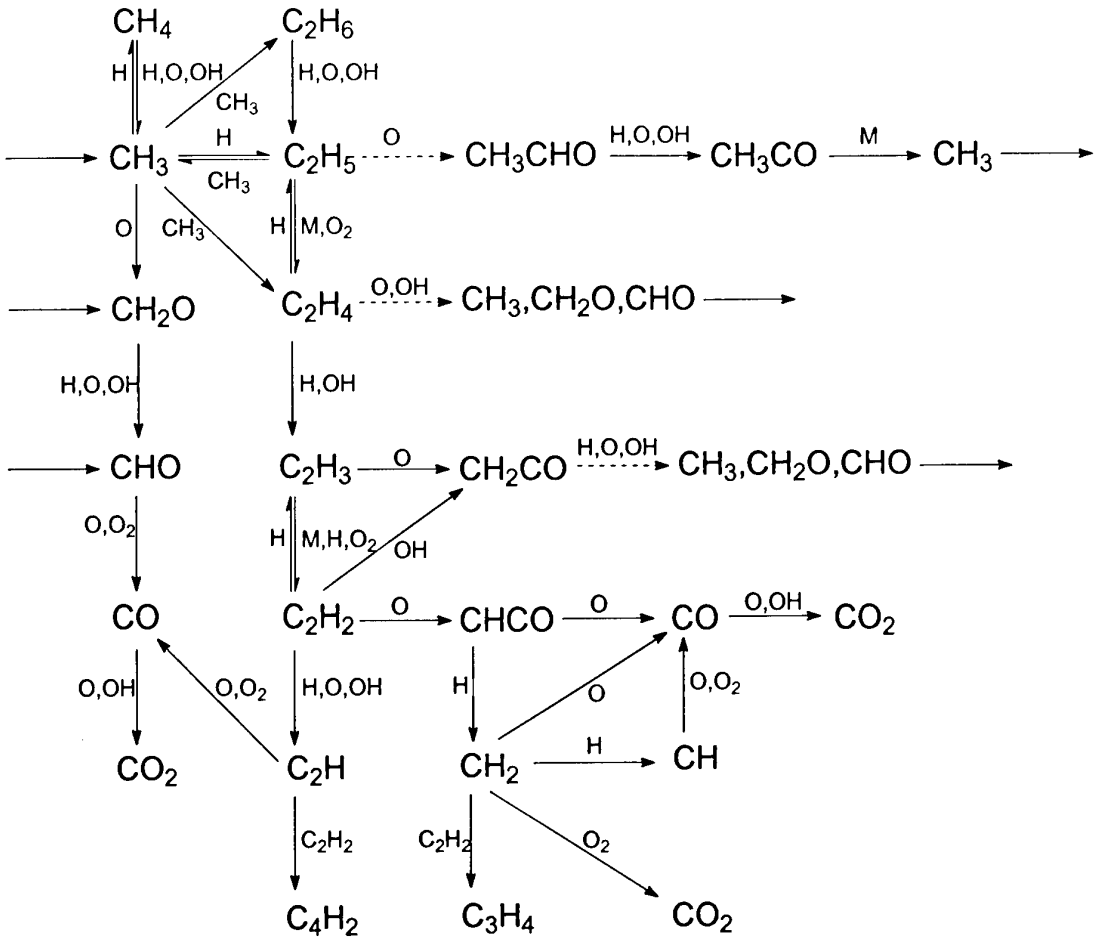

Figure 15. An overview of the high temperature mechanism of the oxidation of aliphatic hydrocarbons at T > 1000 K [Warnatz (1986)]. Degradation of high molecular mass species, such as (1) and (5), eventually lead to the formation of CH_3 and C_2H_5, and partial oxidation generates CH_2O and CHO radicals.

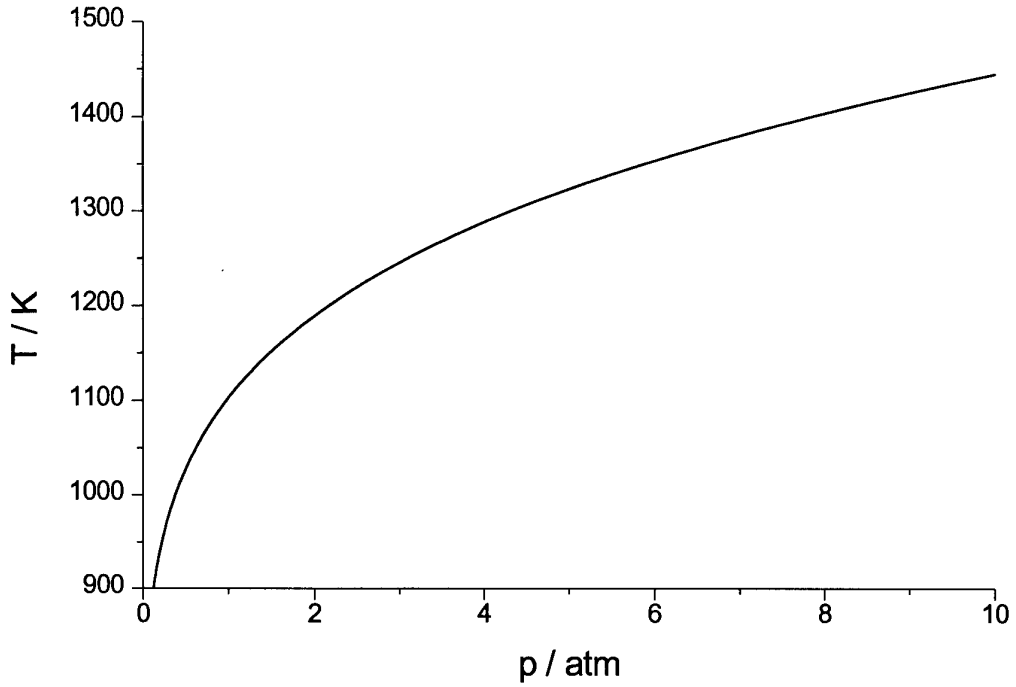

Figure 16. A p-T relationship showing the variation of conditions at which the rates of reactions (64) and (66) are equal. At conditions above the line the branching recation (64) to form OH and O is dominant. At conditions below the line the non-branching reaction to form HO_2 is dominant.

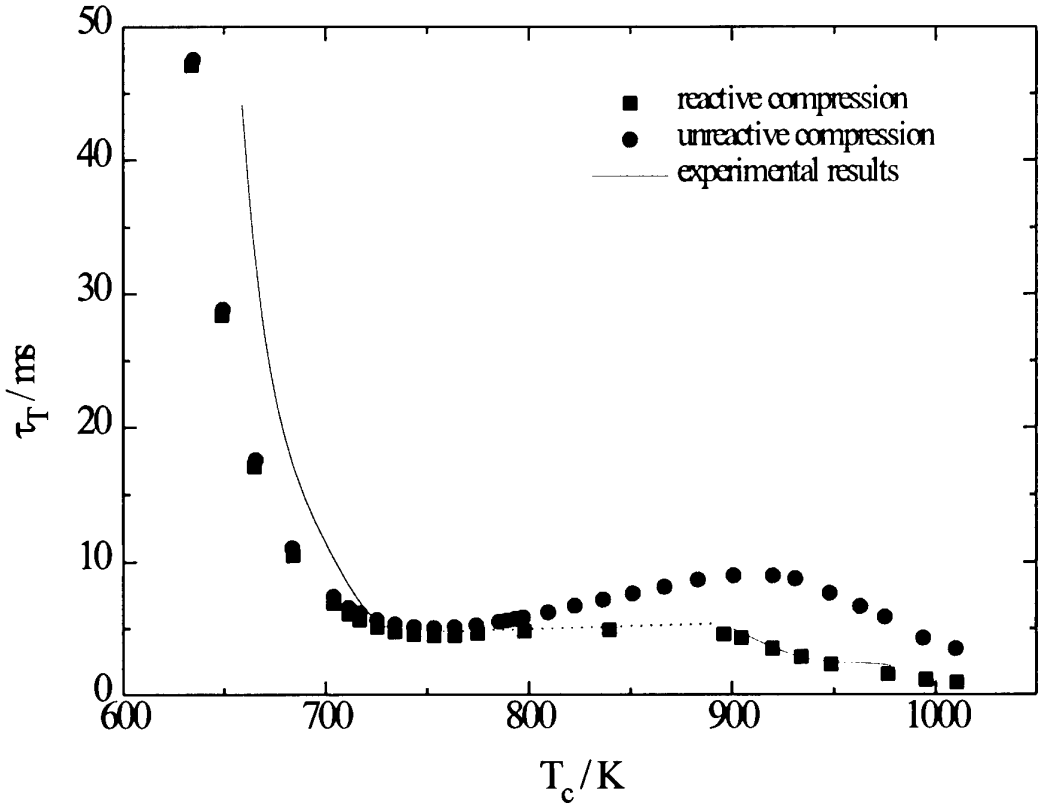

Figure 17 A comparison between the predictions of ignition delay of n-heptane + air mixtures following rapid compression to temperatures in the range 650 - 1000 K at a compressed gas density of 128 mol m^{-3}. The specific pint of interest is that when reaction during the course of compression is taken into account the predicted ignition delay at temperatures above 800 K is considerably shorter than when no such activity is assumed. This indicates how the accumulation of a pool of active species can affect the duration of the ignition delay.

Figure 18 A phase diagram showing the relationship between temperature and reactive species concentrations in the development of chain-thermal ignition. Sensitisation can be brought about by increasing the active species concentration so that the system follows a different trajectory to ignition than would have occurred in their absence. Here the sensitisation is described as the "photochemical path". [Levy *et al* (1969)].

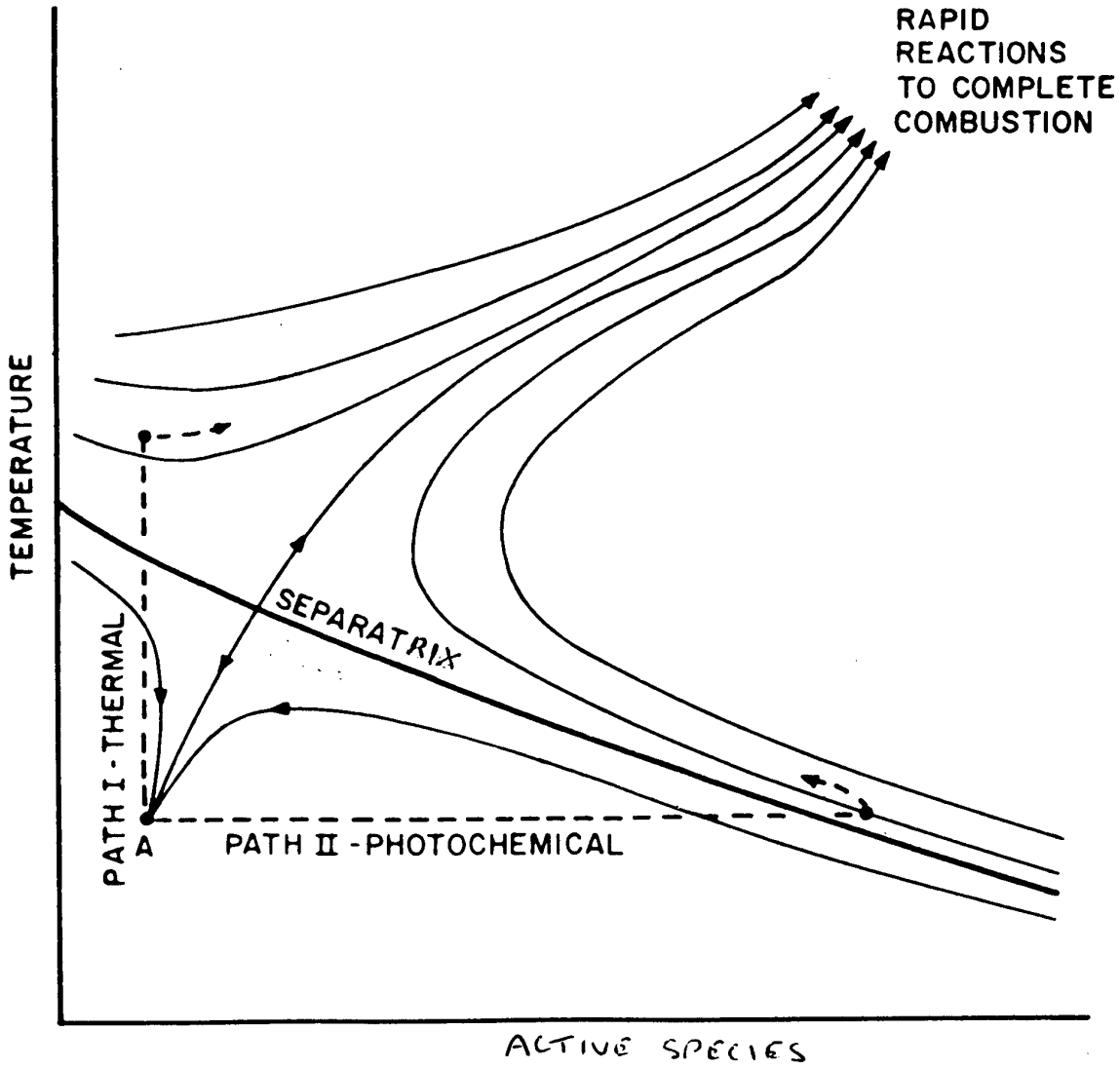

APPENDIX 1. MINIMUM AUTOIGNITION TEMPERATURES (AIT)

The minimum autoignition temperatures of liquid substances are determined by prescribed methods at atmospheric pressure in a thermostated vessel (ASTM-E 659-78, BS 4056, EC - L 251/84) as described in Section 1a. The values given for several homologous series of hydrocarbons are tabulated below. There are marked differences in activity throughout some of these ranges that can be interpreted from the chemical mechanisms described in the main text. The structure of the fuel molecule is the key feature. Reference to the form of the ignition (p T) ignition diagram for aliphatic hydrocarbons is also required in order to understand how discontinuities of the autoignition temperature can arise within a given series.

It is not easy to find comprehensive sets of results that were obtained under the same conditions so that comparisons can be made for different reactants. However, the illustration below, for the combustion of n-hexane and n-butane in air [Kane, G.P., Chamberlain, E.A.C. and Townend, D.T.A., *J. Chem. Soc.*, 435 (1937)], shows not only how at one atmosphere the measured autoignition temperatures can differ by nearly 200 K (points a and b), but also how the autoignition temperature for butane would shift dramatically down by over 100 K if the pressure of the system is raised to several atmospheres (point d). The dependence of autoignition temperature of n-butane on pressure and composition was explored by Chandraratna and Griffiths [*Combust. Flame*, **99**, 626 (1994)]

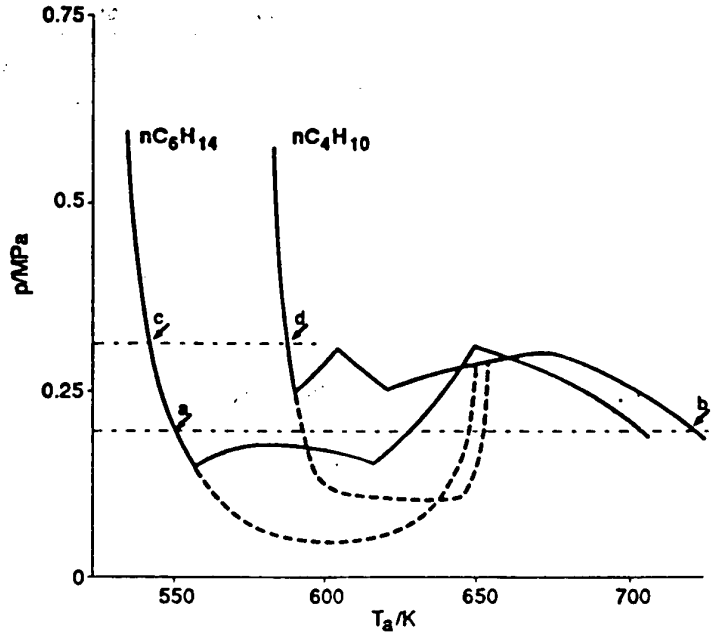

AIT for selected alkanes

alkane	AIT / °C
n-C_4H_{10}	408
n-C_5H_{12}	290
n-C_6H_{14}	248
n-C_7H_{16}	230
n-C_8H_{18}	218
n-C_9H_{20}	205
n-$C_{10}H_{22}$	201-210
n-$C_{12}H_{26}$	200-205/232
n-$C_{14}H_{30}$	200/232
n-$C_{16}H_{34}$	202-205/235
n-$C_{20}H_{42}$	240

C_9 alkane	AIT / °C	C_{10} alkane	AIT / °C
2.2.3.3-tetramethyl pentane	430	2.5.5-trimethylheptane	275
2.3.3.4-tetramethylpentane	437	4.5-dimethylictane	290
3.3.-dimethylheptane	325	2.3-dimethyloctane	225
2-methyloctane	220	2-methylnonane	210
3-methyloctane	220	n-decane	205
4-methyloctane	225		
n-nonane	205		

AIT for selected alkenes

1-alkenes	AIT / °C	octenes[2]	AIT / °C
1-pentene	298	2.4.4-trimethyl-1-pentene	499
1-hexene	272	3.4.4-trimethyl-2-pentene	330
1-heptene	263	2.4.4-trimethyl-2-pentene	308
1-octene	256	2.3.4-trimethyl-1-pentene	256
1-decene	235-244		
1-dodecene	255		
1-tetradecene	239		
1-hexadecene	240		
1-0ctadecene	251		

AIT for selected naphthenes

cyclic alkanes	AIT / °C
cyclopropane	498
cyclopentane	361/380/385
cyclohexane	245/259/270
ethylcyclobutane	211
methylcyclopentane	262/323/329
ethylcyclopentane	265
ethylcyclohexane	262
cyclodecane	235
tetrahydronaphthalene	384/423
decahydronaphthalene	255

AIT for selected aromatics

alkylbenzenes	AIT / °C	di and tri-methylbenzenes	AIT / °C
benzene	592	m-xylene	528/562
toluene	567	p-xylene	528/564
ethylbenzene	460	o-xylene	463/500
n-propylbenzene	456	1.3.5-trimethylbenzene	559
n-butylbenzene	438	1.2.4-trimethylbenzene	520
(naphthalene)	526/587	1.2.3-trimethylbenzene	479

AIT of mixtures

	AIT / °C
gasoline (RON 50/60)	250
kerosene	210-227/295
naphtha (regular)	232
diesel oil	257
gas oil	338
olive oil	441

BIBLIOGRAPHY

Sources of Ignition, J. Bond, Butterworth -Heinemann, London (1991)
J.L. Jackson, *Ind. and Eng. Chem.*, 2869 (1954)
Spontaneous Ignition of Liquid Fuels, B.P. Mullins, Butterworths, London (1954)